CHAPTER 1

Metal Oxide Particles and Their Prospects for Applications

S. Laurent[*,†], S. Boutry[*,†], R.N. Muller[*,†]
[*]University of Mons, Mons, Belgium
[†]Center for Microscopy and Molecular Imaging (CMMI), Gosselies, Belgium

Metal oxides have an important role in a lot of chemical and physical areas. They have attracted many research interests thanks to their physicochemical properties; they have many applications in catalysis [1,2], gas sensing [3], transistors [4], microelectronics [5,6], energy storage and conversion [7,8], environmental decontamination [9], ceramic fabrication [10,11], biomedicine [12–14], and biosensors [15,16]. For example, metal oxides are considered as excellent catalysts because of their acidic and basic properties, which allow to be used as supports for highly dispersed metal catalysts or as precursors of a metal phase [17]. Transition metal oxides (TMOs) can play a key role in numerous reactions as selective oxidation, dehydration, photocatalysis, or electrocatalysis [18–20]. More particularly, TMOs can interact with surfaces of an appropriate carrier to develop monolayer structure of these oxides.

Metal oxide nanostructures can exhibit unique physical and chemical properties due to their limited size that influences basic properties in any material. There are a large variety of metal oxide nanoobjects such as nanoparticles, nanowires, nanotubes, and nanoporous structures [21–27].

If gas-phase processes are successfully employed for the low-cost production of large amounts of nanopowders [28–30], liquid-phase syntheses are more flexible to control the structure, composition, and morphology of the nanomaterials. Liquid-phase ways include coprecipitation, sol-gel processes, hydrothermal methods, template synthesis, or biomimetic approaches [31].

Metal oxides exhibit fascinating electronic and magnetic properties (Table 1.1). For example, some oxides as RuO_2 or ReO_3 are metallic, whereas $BaTiO_3$ is an insulator. The magnetic properties of metal oxides include ferro-, ferri-, or antiferromagnetic behavior. Some oxides possess

Iron Oxide Nanoparticles for Biomedical Applications
https://doi.org/10.1016/B978-0-08-101925-2.00001-2

Table 1.1 Some examples of metal oxide nanoparticles and their applications

Kind of oxide	Properties	Applications	References
Bi_2O_3	Optoelectronic material, semiconductor with photocatalytic activity	Water treatment	[32]
Co_3O_4	Optical, magnetic, and electrochemical properties	Energy storage	[33–35]
CuO, Cu_2O	Optical, electronic material	Antimicrobial agent	[35,36]
Fe_2O_3, Fe_3O_4	Magnetic properties	Biomedical applications—drug delivery, hyperthermia, magnetic resonance imaging (MRI)	[37–40]
Sb_2O_3	Semiconductor material	Chemical catalysis	[41]
SiO_2	Biocompatible properties	Biomedical applications, cosmetics	[42–44]
TiO_2	Electronic properties	Environmental, biomedical applications, photocatalysis	[43,45]
CeO_2	Electronic properties	Antioxidant effects, biomedical applications	[46,47]
UO_2	Electronic properties	Nuclear applications	[48,49]
ZnO	Electronic properties	Decontamination of hydrogen sulfide gas	[50]
ZrO_2	Electro-optical, piezoelectric, and dielectric material	Catalysis applications	[51,52]
SnO_2	Optical and electronic properties	Biomedical applications	[53]

switchable orientation states as in ferroelectrics (titanates, niobates, or tantalates). Other fascinating classes of materials within the metal oxide family are the cuprate superconductors, the manganites showing colossal magnetoresistance or multiferroics combining ferroelectricity and ferromagnetism within the same material ($BiFeO_3$ or $BiMnO_3$) [54].

The other most widely used nanoparticles are TiO_2 (titania), ZrO_2 (zirconia), CeO_2 (ceria), or Fe_2O_3 and Fe_3O_4 (magnetic iron oxides). These materials present catalytic, antioxidant, and bacterial activities; good stability; and biocompatibility. They are used for numerous biomedical applications such as therapeutic and diagnostic agents, components in medical implants or drug delivery [55–60]. For example, titania with a biocompatible surface for cells and their proliferation is often used in medical implants [61,62]; magnetic iron oxides are reported for cell labeling, magnetic resonance imaging (MRI), and targeted drug delivery [63,64]; ceria is known for its catalytic and antioxidant activity [65–67].

Many reviews on the synthesis, characterization, and applications of metal oxides have been published [68–70]. Preparation of uniform nanoparticles with different controlled shapes has been described [71–78]. The physicochemical properties of the nanosystems can be tuned by changing the nature of the precursor or solvent or the experimental conditions. A stabilizer can be used during the synthesis of the nanoparticles (in situ synthesis or one-pot synthesis) or added to the already formed particles using adsorption, chemical grafting, or ligand exchange (postsynthesis). They are usually large molecules with functional groups that can be chemically or physically adsorbed on the particle surface, such as polysaccharides, polyvinyl alcohol, polyacrylamides, silica, or gold layer onto the particle surface (Fig. 1.1).

A lot of biomedical applications need surface modification with fluorophores and biological vectors (as peptides, organic mimetics, antibodies, or proteins) for targeted molecular imaging. Different strategies have been developed to obtain nanostructures with multiple functions on the surface (Fig. 1.2): drug carrier, biovectors, imaging probes, and molecules to enhance biocompatibility or to improve intracellular behavior [79].

Coated nanoobjects can modify the behavior of the bare nanoparticles in a biological media. In fact, the interaction with proteins, cells, or tissues depends of the surface chemistry [80–87]. Thus, potential zeta, nature of the coating, particle composition, aggregation, shape, and size can change the in vivo behavior: cellular uptake, toxicity, biodistribution, clearance, etc. [57,85,88–91].

The characterization of the modified surface nanoparticles can be performed by various techniques as zeta potential (particle charge surface), dynamic light scattering (particle size distribution), transmission electron microscopy (size of the crystal), X-ray diffraction (composition of the core), FTIR spectroscopy, TOF-SIMS, and XPS (the presence of functional groups) [8].

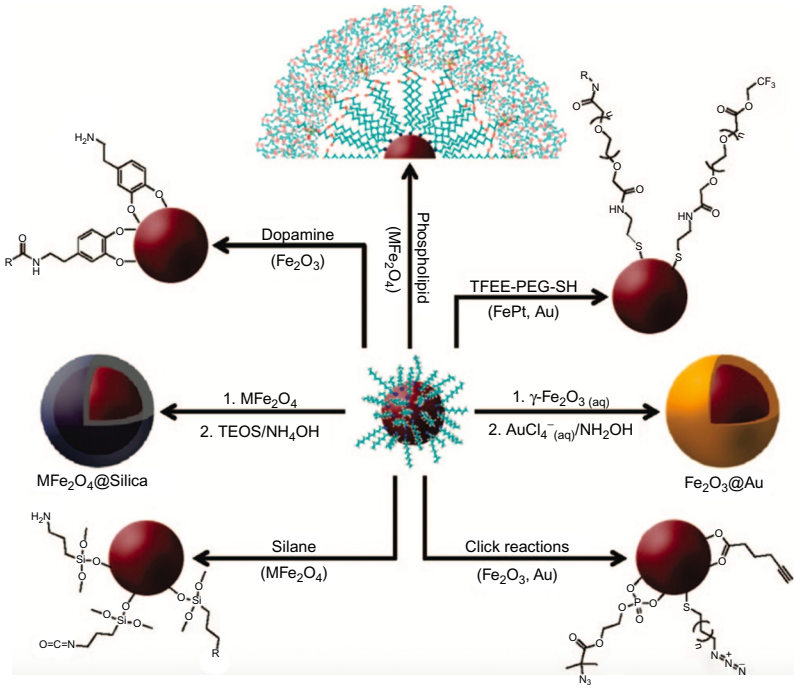

Fig. 1.1 Different ways of stabilization of iron oxide nanoparticles. *Reprinted with permission from A.H. Latham, M.E. Williams, Controlling transport and chemical functionality of magnetic nanoparticles, Acc. Chem. Res. 41(3) (2008) 411–420. Copyright 2008, American Chemical Society.*

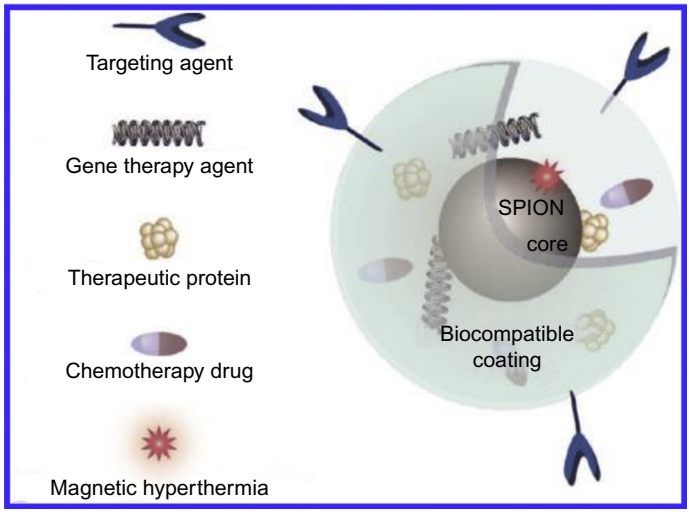

Fig. 1.2 Surface modification of iron oxide nanoparticles. *Reprinted with permission from F.M. Kievit, M. Zhang, Surface engineering of iron oxide nanoparticles for targeted cancer therapy, Acc. Chem. Res. 44(10) (2011) 853–862. Copyright 2011, American Chemical Society.*

Interactions between nanoparticles and proteins can occur on the nanoparticle surface; protein can cover the particle and form a protein corona [92–94]. The composition of this protein corona can influence the transport and the biodistribution of the particles. Metal oxide nanoparticles (TiO_2, SiO_2, and ZnO) can be bound to different plasma proteins [95]. A method to avoid this protein adsorption is to coat the nanoobjects with a polyethylene glycol (PEG) derivative; this polymer layer creates a protective shell around nanoparticles. Metal oxides present excellent magnetic and photoluminescent properties.

1.1 MAGNETIC METAL OXIDES

The magnetic properties are determined by the orientation and the number of the electron spins. In the case of TMOs, the individual electrons are strongly correlated in their motion, and the spin of an ion is characterized by one global atomic spin. The atomic spins of neighboring ions may also be strongly correlated to form a spin sublattice. Following the magnitude, the orientation, and the number of spin sublattices, metal oxides possess different magnetic fields and different responses when an external magnetic field is applied (Table 1.2) [96].

There are different types of magnetism: dia-, para-, antiferro-, ferri-, and superparamagnetism. The behavior of small oxide nanoparticles differs from the bulk behavior due to the large contribution from atoms on the surface. The surface atoms may have different atomic spins than the bulk ions if they are in a different oxidation state. The magnetic susceptibilities of some antiferromagnetic oxides as Fe_2O_3, NiO, or CoO have been measured at different temperatures for different crystal sizes [97–102]. For small sizes (less than 14 nm), the magnetic susceptibility increases, and it decreases with increasing temperatures. This is a typical behavior for superparamagnetic particles.

Some properties of magnetic metal oxide nanoparticles are suitable for sensor applications. Magnetic responses, as coercivity changes, are based on fundamental properties of magnetic metal oxide nanoparticles [103–107]. In the case of magnetostrictive sensor, changes in position are monitored. The principal advantage of this system is the absence of physical contact.

Magnetic metal oxide nanoparticles are of great interest in biomedicine due to the ability to manipulate the particles with an external magnetic field [108–110]. The ability to control the delivery of drugs using a magnetic field

Table 1.2 Room-temperature magnetic properties of some transition metal oxides [96]

Magnetic properties	Diamagnetic	Paramagnetic	Antiferromagnetic	Ferrimagnetic
Metal oxides	Sc_2O_3 Y_2O_3 TiO_2 V_2O_5 CrO_3 Nd_2O_3 AgO HgO Ta_2O_5	Ti_2O_3 VO VO_2 NdO_2	Cr_2O_3 MnO Mn_2O_3 MnO_2 FeO α-Fe_2O_3 CoO NiO V_2O_3	Mn_3O_4 Fe_3O_4 γ-Fe_2O_3

has generated a lot of interest. Other applications of these magnetic nanoparticles include cell separations/extractions and cell/drug manipulations via magnetic fields.

MRI is another area in biomedicine that has benefited from the application of magnetic metal oxide nanoparticles. MRI is a powerful noninvasive tool used in medicine but suffers from low signal sensitivity. The use of contrast agents helps in this but suffers from their own drawbacks. The most common contrast agents used are paramagnetic materials that utilize T_1 relaxation (called spin-lattice relaxation time, it is related to the mechanism by which the component of the magnetization vector along the direction of the static magnetic field reaches thermodynamic equilibrium with its surroundings). Superparamagnetic metal oxides, such as Fe_3O_4, effects T_2 relaxation times (called spin-spin relaxation time, it is related to the time of relaxation of protons interfering with each other) by altering local magnetic fields surrounding protons.

A third interesting application of metal oxide nanoparticles is hyperthermia treatment, using a magnetic field to heat up magnetic nanoparticles. Localized heating in specific locations can be achieved through the use of an alternating magnetic field and magnetic nanoparticles. The nanoparticles heat up due to reversal of magnetic spins within the nanoparticles or physical rotation of the nanoparticles in a viscous solution. Magnetic hyperthermia is being investigated for its application into the treatment of cancer treatment.

A lot of applications of magnetic iron oxide nanoparticles as Fe_2O_3 or Fe_3O_4 are known in the biomedical field as (i) cell labeling, (ii) MRI, (iii) targeted drug delivery, (iv) hyperthermia, and (v) biosensing [111–113]. Another example is MnO nanoparticles obtained by thermal

decomposition of Mn oleate complex and encapsulated in a polyethylene glycol-phospholipid shell [114]. These nanoobjects gave a bright signal in T_1-weighted MR images.

Nanoparticles are promising for numerous biomedical applications thanks to their optical and magnetic properties. For example, semiconductor nanoparticles are used as fluorescence probes for labeling and optical imaging of biological tissues [115,116].

1.2 METAL OXIDES WITH PHOTOLUMINESCENCE PROPERTIES

ZnO, SnO_2, and In_2O_3 metal oxide nanostructures have been studied a lot for their numerous applications [117–123]. Among them, the wide-bandgap semiconducting oxide nanoobjects with photoluminescence in blue light and ultraviolet have an important role in laser printing, information storage, or nanoscale optoelectronic devices. If the bulk In_2O_3 cannot emit light at room temperature [124], the emission spectrum recorded from In_2O_3 nanowires showed a strong photoluminescence peak at 490 nm [125]. Following the shape of In_2O_3 nanostructures, different peaks can be observed. For example, nanowires have peaks centered at 425, 429, 442, and 460 nm [126], 298 nm [127], or 416 and 435 nm [128]; nanocubes have peaks centered at 450 nm [129]. These photoluminescence peaks in the visible emission are attributed to the oxygen vacancies and emission results from the recombination of a photoexcited hole with an electron occupying the oxygen vacancies [130]. Similar behavior is reported for SnO_2 nanosystems. For SnO_2 nanowires, the emission peak is centered at 602 nm, for SnO_2 nanoblades, the peak is centered at 445 nm, and for SnO_2 nanoribbons, the emission is observed at 500 nm [131–133].

For different ZnO nanostructures, different emissions have been also reported [134–139]. For ZnO, In_2O_3, SnO_2 and many other nanostructures, such as ZrO_2 nanowires, many authors explained that the origin of strong emission in visible emission is due to oxygen vacancies produced in the growth of nanomaterial [125–132,134–136,140].

Some articles describing the preparation of rare-earth oxide and their physicochemical properties have been published [141–143].

In the following parts of this chapter, the different properties of metal oxide nanoparticles will be highlighted in numerous applications: electronics, catalysis, gas sensing, energy technologies, and finally biomedical applications as MRI, cancer treatment, and biomedical implant.

1.3 METAL OXIDES IN ELECTRONICS, CATALYSIS, GAS SENSORS AND ENERGY TECHNOLOGIES

1.3.1 Metal Oxide in Electronics

Complex metal oxides, exhibiting strong structure-composition-property relationships, like perovskite (e.g., $SrTiO_3$, $SrRuO_3$, or $PbTiO_3$), show excellent properties as insulating, ferroelectric behavior, magnetoresistance, or high-temperature superconductivity [144]. In these materials, charge, spin, and orbital degrees of freedom couple with dynamic lattice effects present a rich base for fundamental and applied researches [145].

Vanadium dioxide, VO_2, is one of the most studied correlated electron systems that exhibits a metal-insulator transition (MIT) near room temperature (~67°C). The phenomenon of MIT phase transition in strongly correlated electron systems is one of the focus areas of research in condensed matter physics [146]. The interest is partly motivated by the potential of the materials exhibiting an MIT to be used in novel electronics and electro-optical applications as switches or memory elements [147–150]. There is a considerable interest in understanding the fundamental science behind the correlated electron behavior responsible for striking material property changes such as a MIT, high-temperature superconductivity, and magnetoresistance.

Lu et al. studied magnetic oxide thin-film properties and specially their utilities in spintronics devices. The term "spintronics" usually refers to the manipulation, storage, and transfer of information by means of electron spins in addition to or in place of the electron charge as in conventional electronics. Spintronics promises the possibility of integrating memory and logic into a single device [151]. Oxides with the same crystal structure can possess very different physical properties following the constituents and doping; these oxides can be used as building blocks to construct heterostructures that can function as magnetic tunnel junctions, spin valves, etc. Oxide spintronics has become an active research area that can find scientific and technological impact [152]. Recently, many new phenomena including magnetic ordering have been observed at the interface between two perovskite oxides mostly on $SrTiO_3$ and $LaAlO_3$ that make it feasible to build interface devices [153,154].

Multiferroic is used to describe materials that possess two or all three of the ferroproperties: ferroelectricity, ferro-/ferrimagnetism, and ferroelasticity. In a broader sense, it also covers materials with ferro- and antiferroproperties or pure antiferroproperties. These materials have been known for

decades; however, interest in multiferroics has been revitalized in the past few years largely due to the advancements in both first principle calculations and experimental techniques, especially in thin-film growth [155]. Multiferroic materials play a significant role in developing systems with large magnetoelectric coupling where the manipulation of magnetization or polarization can be achieved by applying an electric or magnetic field, respectively. This magnetoelectric coupling with an extra degree of freedom will eventually usher a paradigm shift from conventional electronic devices. Many have already proposed novel device concepts based on multiferroic [156–158]. $BiFeO_3$ is the most studied multiferroic materials because of its room-temperature antiferromagnetism and ferroelectricity (Fig. 1.3) [159,160].

Ferroelectrics form an important class of materials with giant electromechanical and dielectric response properties, which are crucial in technologies ranging from microelectromechanical systems to computer memory devices. Ferroelectrics exhibit a spontaneous electric polarization (electric dipole moment per unit volume) that can be *switched* with large enough external fields to its symmetry equivalent states, in particular to the one with reversed direction. Fundamentally, the strong coupling of spontaneous polarization with external stress and electric fields is linked with a structural (or ferroelectric) phase transition exhibited by ferroelectrics as a function of temperature, which depends sensitively on applied stress and electric fields. The coupling between the polarization and stress facilitates their use as sensors and actuators, and the dielectric coupling and switchability of polarization facilitate their use in memory devices. Some examples of perovskite ferroelectrics are $KNbO_3$, $BaTiO_3$, $PbTiO_3$, and $BiAlO_3$. These materials are ferroelectric above room temperature and become paraelectric above a ferroelectric transition temperature [161–163].

Very recently, Yu et al. have summarized the different optoelectronic applications of metal oxides. They have compared the traditional inorganic semiconductors as silicon and the metal oxides in terms of electronic structure, charge transport mechanisms, defect states, thin-film processing, and optoelectronic properties [164].

1.3.2 Metal Oxides as Catalysts

Metal oxides are used as catalysts for industrial chemical synthesis thanks to their ability to participate in acid-base and redox reactions [165,166]. For example, TMOs, such as MnO or Mn_3O_4, are used extensively in industry

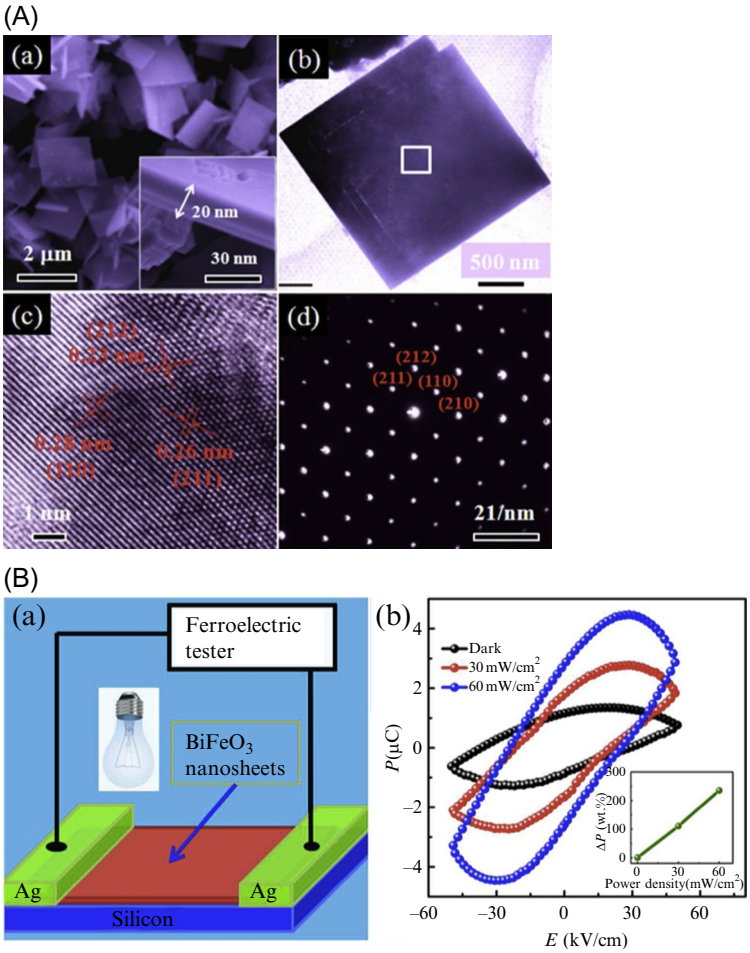

Fig. 1.3 (A) SEM image of $BiFeO_3$ nanosheets showing $BiFeO_3$ nanosheet is square with 20 nm thickness (a), TEM image of individual $BiFeO_3$ nanosheets showing that the individual $BiFeO_3$ nanosheets present about 4 μm^2 of area (b), HRTEM image of a typical portion corresponding to the rectangular area of part b (c), SAED pattern of $BiFeO_3$ nanosheets indicating that the $BiFeO_3$ nanosheets have an excellent structure (d). (B) Light-induced change of the ferroelectric polarization of $BiFeO_3$ nanosheets. A schematic diagram of the circuit used for the P-E hysteresis measurements, where the $BiFeO_3$ nanosheets lay on an insulated silicon substrate and Ag acts as two electrodes (a), P-E hysteresis loops (b) obtained at 100 Hz illuminated under an ordinary filament lamp with different power densities at room temperature (300 K). Inset to (B): the light-power-density-dependent ΔP. *Reprinted with permission from B. Sun, P. Han, W. Zhao, Y. Liu, P. Chen, White-light-controlled magnetic and ferroelectric properties in multiferroic $BiFeO_3$ square nanosheets, J. Phys. Chem. C 118(32) (2014) 18814–18819. Copyright 2008, American Chemical Society.*

for the selective oxidation of hydrocarbons. Since the site of the oxidation reactions occurs at surface oxygens, metal oxide nanoparticles, with an increased ratio of surface area to volume, become more efficient. If the metal oxide were immobilized on a magnetic core, collection and separation of the catalyst from the reactional mixture become more efficient with a magnetic field [167].

Recycling catalysts is of particular interest, especially if the catalyst is expensive. Immobilization of catalysts on micrometer material has been used for many years now and allows for the separation of the catalyst from product via a filtration process. A way to improve this separation efficiency is to use magnetic nanoparticles. Again, due to their high surface area, the loading of catalysts is much higher and allows for easier access to the catalysts' active sites. Another advantage of the use of magnetic nanoparticle catalyst supports is the ability to "turn off" a reaction by moving the catalysts out of the reaction with an applied magnetic field. This also allows for the easy recovery of the catalyst at the end of the reaction.

The most active metal oxide catalysts for complete oxidation for a variety of reactions are oxides of Ag, V, Mn, Fe, CO, Cu, or Ni [168–171]. CuO is also known to be an effective catalyst of oxidation [172,173] and is considered as a substitute for noble metal catalysts in emission control applications due to its high activity tolerance to sulfur [174]. Among the TMOs, Mn oxides are recognized as being very active for total oxidation of CO [175,176]. They are considered as nontoxic for the environment [177] and possess the necessary electron-mobile environment for optimal surface redox catalysts. In fact, Mn oxide can present Mn atoms with different oxidation states [178]. Commercial catalysts based on Mn oxides are also used in self-cleaning oven walls [179].

Recently, Asano et al. have reported that metal oxide-supported Pt-MoO_x catalysts are effective for hydrogenation of 2-furancarboxylic acid to valeric acid in water solvent. These catalytic systems allowed the hydrogenation of 2,5-furandicarboxylic acid (Fig. 1.4) [180].

1.3.3 Metal Oxides in Gas Sensing

A gas sensor can be defined as a device giving information about the composition of the ambient atmosphere. Upon interaction with chemical species (adsorption, chemical reaction, or charge transfer), the physiological properties of the metal oxide layer are modified. These changes are translated into electric signals.

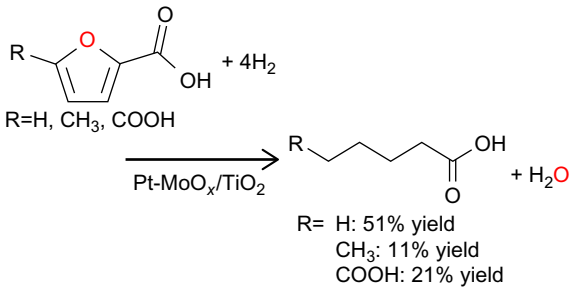

Fig. 1.4 Hydrogenation with Pt-MoO_x/TiO_2 as catalyst. *Reprinted with permission from T. Asano, M. Tamura, Y. Nakagawa, K. Tomishige, Selective hydrodeoxygenation of 2-furancarboxylic acid to valeric acid over molybdenum-oxide-modified platinum catalyst, ACS Sustain. Chem. Eng. https://doi.org/10.1021/acssuschemeng.6b01640 (Accepted Manuscript). Copyright 2016, American Chemical Society.*

Semiconductor oxide-based gas sensors are classified according to the direction of the conductance change due to the exposure to reducing gases as n-type (conductance increases, e.g., In_2O_3, ZnO, or SnO_2) or p-type (conductance decreases, e.g., Cr_2O_3 or CuO). This classification is related to the conductivity type of the oxides, which is determined by the nature of the dominant charge carriers at the surface, that is, electrons or holes. Based on the electronic structure, metal oxide semiconductor (MOS) elements like Cr_2O_3, ZnO, SnO_2, Mn_2O_3, Co_3O_4, NiO, CuO, SrO, In_2O_3, WO_3, TiO_2, V_2O_3, Fe_2O_3, GeO_2, Nb_2O_5, MoO_3, Ta_2O_5, La_2O_3, CeO_2, and Nd_2O_3 are suitable for detecting reducing or oxidizing gases through conductive measurements.

Only TMOs with d^0 and d^{10} electronic configurations find their real gas-sensing application. The d^0 configuration is found in binary TMOs such as TiO_2 and V_2O_5, while d^{10} configuration is found in post-TMOs, such as ZnO and SnO_2. Among different materials studied for gas-sensing applications, SnO_2 and ZnO are the most extensively studied compared with other metal oxides. Their use as a gas sensor, in which the surface conductivity changes in response to adsorbed gases, made them an ideal candidate in the field of surface science.

There are different types of gas sensors: (i) capacitance-based gas sensors, based on a change in dielectric constant of films between the electrodes as a function of the gas concentration; (ii) acoustic-wave-based gas sensors, based on using piezoelectric material that has one or more transducers on its surface; (iii) calorimetric gas sensors, based on change in temperature on catalytic surfaces; (iv) optical gas sensors, based on an absorbance on exposure to

the analyte; and (v) electrochemical gas sensors, based on the measurement of the concentration of a target gas by oxidizing or reducing the target gas at an electrode and measuring the resulting current.

Many researches on metal oxide gas sensors have been published [181–199]. Many metal oxides are suitable for detecting combustible, reducing, or oxidizing gases by conductive measurements. The following oxides show a gas response in their conductivity: Cr_2O_3, Mn_2O_3, Co_3O_4, NiO, CuO, SrO, In_2O_3, WO_3, TiO_2, V_2O_3, Fe_2O_3, GeO_2, Nb_2O_5, MoO_3, Ta_2O_5, La_2O_3, CeO_2, and Nd_2O_3 [200].

The range of electronic structures of oxides are so wide that metal oxides were divided into the following two categories [180,201]:

(1) TMOs (Fe_2O_3, NiO, Cr_2O_3, etc.)

(2) Non-TMOs, which include pre-TMOs (Al_2O_3, etc.) or post-TMOs (ZnO, SnO_2, etc.)

Gas sensors based on the MOSs have been used to detect numerous gases as CO_2, CO, NO_2, CH_4, ethanol, LPG. They have been studied due to their advantages: low cost, simplicity, small size, and high compatibility with microelectronic processing [202]. They have many applications in different areas such as in environment, home safety, and industry [203,204].

Various morphologies of MOS nanostructures (wirelike, belt-like, rodlike, or tetrapods) have been investigated for gas-sensing applications. One-dimensional nanostructures such as nanowires, nanobelts, and nanoneedles have gained a lot of interest for nanodevice design and fabrication [205,206].

The fundamental mechanism of gas sensing based on MOS depends on the reaction between reactive chemical species (O^-, O^{2-}, H^+, or OH^-), the sensor surface and the gas molecules (reducing/oxidizing gas) to be detected [207]. Thus, it is important to understand the surface reactions between semiconductor surface and target gas for improving the sensing characteristics. Typically, the important parameters in sensor development are sensitivity, selectivity, and stability [208–210].

A lot of MOS are based on SnO_2, TiO_2, WO_3, In_2O_3, ZnO, or Fe_2O_3. Noble metals such as Au, Pt, Pd, and Ag on the surface of MOS can act as a catalyst to modify surface reactions of MOS toward sensing gas and result in high sensitivity.

Resistive chemical sensors are devices in which the electric transport properties of the MOS sensing layer are modified by contact with reducing or oxidizing gases. The gas-sensing efficiency of MOS changes between bulk and nanostructured forms. In fact, the same material with different sizes

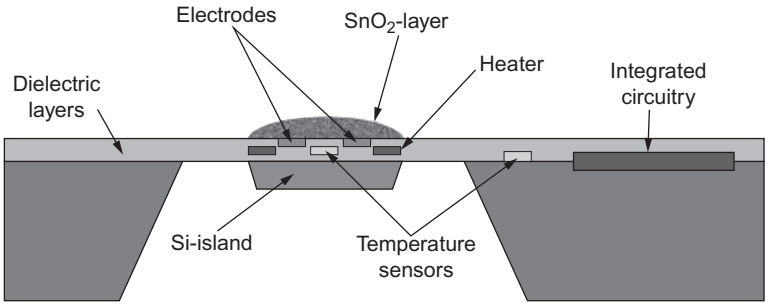

Fig. 1.5 Schematic cross section of the sensor chip developed by Graf et al. *Reprinted with permission from M. Graf, Diego B.S. Taschini, C. Hagleitner, A. Hierlemann, H. Baltes, Metal oxide-based monolithic complementary metal oxide semiconductor gas sensor microsystem, Anal. Chem. 6 (2004) 4437–4445. Copyright 2004, American Chemical Society.*

and shapes shows different electric [211,212], sensing [213–215], or catalytic behaviors [216]. Graf et al. presented a fully integrated gas sensor microsystem with a micro hot plate and an analog and digital circuitry on a single chip [217]. The micro hot plate is coated with a nanocrystalline SnO_2 thick film (Fig. 1.5). Traces of CO in very low concentration (subparts-per-million range) are detectable.

1.3.4 Metal Oxide in Energy Technologies

Renewable energy, as solar energy, is very important for our society due to the increasing demand. Solar cells allow to transform solar energy into electric energy. Silicon-based solar cells are currently the dominant technology, with high power conversion efficiency (PCE) and stability, but they are relatively expensive. Organic-inorganic hybrid perovskite solar cells (PSCs) are the most promising next-generation photovoltaic technologies due to their high PCE, low cost, and easy fabrication [218].

A fine morphological distribution of two types of materials (electron donor and electron acceptor) within one layer is essential for good device performance. The advantage of hybrid organic solar cells (OSCs) is the stability and controllability of the morphology of the active layer. The morphology of ZnO-polymer hybrid solar cells is for a large part controlled by choosing the hydrophilicity of the polymer [219]. When this polymer is functionalized with ester functions, increasing the hydrophilicity, the ZnO shows a much finer distribution across the layer. In thin active layers, the finer morphology leads to an enhancement of device performance.

Increasing effort is being applied to develop multifunctional solar cells that integrate new capabilities for creating various or neutral colors in a desired manner, thereby opening up the possibility of numerous applications, including building-integrated photovoltaic (BIPV) systems, photon energy conversions, tandem cells, wearable electronics, and energy-saving colored display technologies [220–237]. Lee et al. have summarized recent works on PSCs with neutral-colored and multicolored semitransparency for BIPVs and tandem solar cells [238].

In photovoltaics, MOS serves as a scaffold layer for loading dyes in dye-sensitized solar cells (DSSCs) and organic-inorganic hybrid perovskites in PSCs and electron and hole transport layers in DSSC and OSCs. The function of scaffold in DSSC is to facilitate charge separation and charge transport, whereas that of the transport layers is to conduct one type of charge carrier block to the other type [239]. Therefore, tailoring their properties is inevitable to develop high-performing photovoltaic devices using them. On the other hand, the electrochemical properties of the MOS such as band-edge energies determine their success as photocatalysts.

Wang et al. developed a self-assembly approach to prepare metal oxide-graphene nanocomposites with well-controlled nanostructures [240]. This class of layered nanocomposites contains stable, ordered, alternating layers of nanocrystalline metal oxide and graphene-graphene stacks (Fig. 1.6). The graphene materials can also be incorporated into hexagonal nanostructures to form high-surface-area, conductive porous networks for energy storage. SnO_2-graphene nanocomposite films displayed near theoretical specific energy density for Li ion insertion/extraction without significant charge/discharge degradation.

1.4 METAL OXIDES IN BIOMEDICAL APPLICATIONS

1.4.1 MRI and Cancer Treatment

MRI is based on the same principle than the one used in chemical nuclear magnetic resonance (NMR) analysis and is one of the most useful diagnostic imaging techniques thanks to its excellent spatial resolution and noninvasive nature. For improved imaging quality including sensitivity, resolution, tissue, or organ specificity, contrast agents are generally required. Considerable attention has been given to develop various nanosized contrast agents, since conventional low-molecular-weight agents (like Gd-DTPA and Gd-DOTA derivatives) possess disadvantages such as rapid excretion [241], relatively low contrast efficiency [242], potential renal toxicity

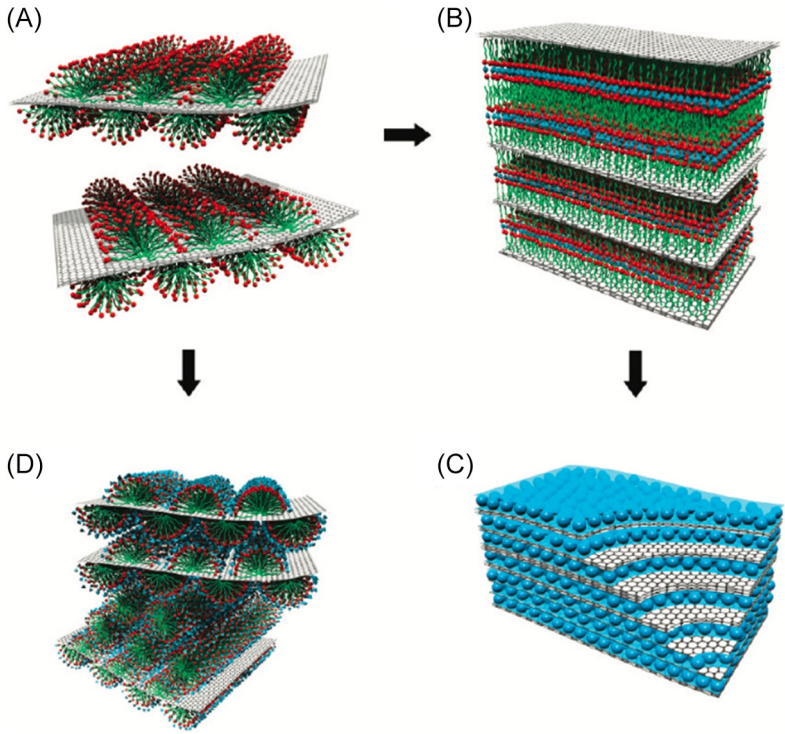

Fig. 1.6 Schematic illustrations of the ternary self-assembly approach to ordered metal oxide-graphene nanocomposites. Graphene or graphene stacks, which are used as the substrate instead of graphite. Adsorption of surfactant hemimicelles on the surfaces of the graphene or graphene stacks causes its dispersion in surfactant micelles in an aqueous solution (A), the self-assembly of anionic sulfonate surfactant on the graphene surface with oppositely charged metal cation species and the transition into the lamella mesophase toward the formation of SnO_2-graphene nanocomposites, where hydrophobic graphenes are sandwiched in the hydrophobic domains of the anionic surfactant (B), metal oxide-graphene layered nanocomposites composed of alternating layers of metal oxide nanocrystals and graphene/graphene stacks after crystallization of metal oxide and removal of the surfactant (C), self-assembled hexagonal nanostructure of metal oxide precursor (e.g., silicate) with nonionic surfactants (e.g., Pluronic P123) on graphene stacks (D). *Reprinted with permission from M. Graf, Diego B.S. Taschini, C. Hagleitner, A. Hierlemann, H. Baltes, Metal oxide-based monolithic complementary metal oxide semiconductor gas sensor microsystem, Anal. Chem. 6 (2004) 4437–4445. Copyright 2010, American Chemical Society.*

[243], and the lack of specificity to target disease or cancerous tissues [244]. MRI is highly useful for diagnosis and therapy monitoring [245]. The latter provide an excellent soft-tissue contrast, which enables the noninvasive and highly accurate detection of, that is, tumors and inflammation sites.

The parameters that define the efficiency of as an MRI contrast agent are the longitudinal (r_1) and transversal (r_2) relaxivities. These proton relaxivities give the efficacy of magnetic nanoparticles to increase the longitudinal (R_1) or transversal (R_2) relaxation rate of water protons induced by one millimolar of iron (Eq. 1.1):

$$R_i^{\text{obs}} = \frac{1}{T_i^{\text{obs}}} = \frac{1}{T_i^{\text{dia}}} + r_i \cdot C \quad (i = 1 \text{ or } 2) \tag{1.1}$$

where R_i^{obs} is the global relaxation rate of the system (s^{-1}), T_i^{obs} is the global relaxation time of the system, T_i^{dia} is the relaxation time of the system before the addition of the contrast agent (s), C is the iron concentration of the superparamagnetic compound (mmol L^{-1}), and r_i is the relaxivity.

The evolution of longitudinal relaxivity as a function of external magnetic field is shown by nuclear magnetic resonance dispersion (NMRD) profiles [40] (Fig. 1.7).

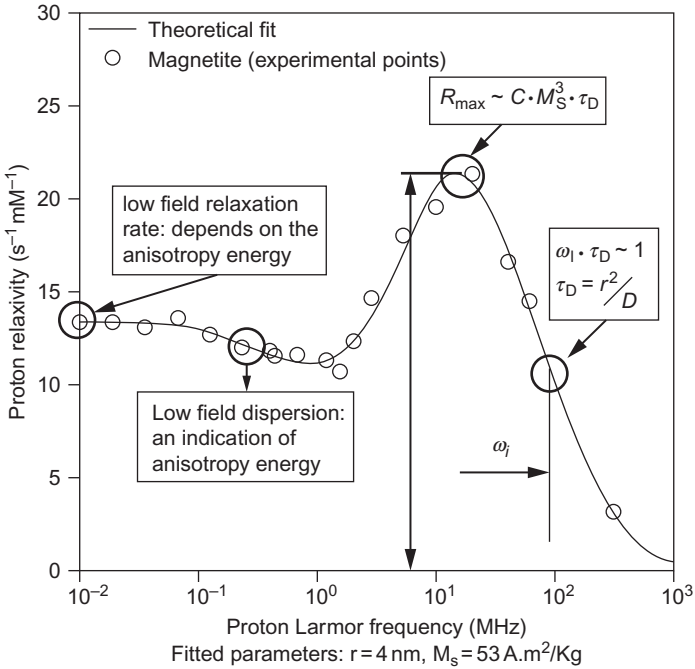

Fig. 1.7 NMRD profile of magnetite particles in colloidal solution. *Reprinted with permission from S. Laurent, D. Forge, M. Port, A. Roch, C. Robic, L. Vander Elst, R.N. Muller, Magnetic iron oxide nanoparticles: synthesis, stabilization, vectorization, physicochemical characterizations and biological applications, Chem. Rev. 108(6) (2008) 2064–2110. Copyright 2008, American Chemical Society.*

The fitting of the NMRD profiles by adequate theories gives information about the nanocrystals, their average radius r, their specific magnetization M_s, their anisotropy energy E_a, and their Néel relaxation time τ_N.

Different methods can be used to determine nanoparticle characteristics. The size of the particle core can be determined by TEM images. It provides details on the size distribution and the shape. XRD can be performed to obtain the crystalline structure of the particles. In a diffraction pattern, the intensity can be used to quantify the proportion of iron oxide formed in a mixture by comparing experimental peak and reference peak intensities [246]. The crystal size can be calculated also from the line broadening from the XRD pattern using the Scherrer formula [247]. Dynamic light scattering (DLS) is a common technique to obtain the hydrodynamic sphere of nanoparticles. Additionally, magnetometry and relaxivity properties recorded over a wide range of magnetic fields can be used to determine the mean crystal size, among numerous other parameters. Other physicochemical techniques, such as atomic-force microscopy (AFM), thermogravimetric analysis (TGA), differential scanning calorimetry (DSC), X-ray photoelectron spectroscopy (XPS), Fourier transform infrared spectroscopy (FTIR), secondary ion mass spectra (SSIMS and TOF-SIMS), conductometry, potentiometry, and solid-state NMR, have been used to investigate the surface properties of coated IONPs. It is worth noting that some of these techniques are used to describe the nature and strength of the bonding between the iron oxide surface and the coating, while others are used to understand the coating influence on the nanoparticle magnetic properties.

The blood half-life, opsonization, biokinetics, and biodistribution of nanoparticles are determined by the surface chemical nature and the particle size. To be used in the biomedical field, there are some requirements as hydrophilicity and biocompatibility, furtivity, colloidal stability in water and protein-rich physiological media, and a hydrodynamic size < 100 nm.

NPs shape, structure, composition, synthesis method, and coating play a crucial role in the nontoxicity, biocompatibility, stability, reticuloendothelial system (RES) escape, internalization by cancer cells, and MRI properties of iron oxide nanoparticles [248,249].

Most iron oxide nanoparticles usually used in preclinical or clinical tests are coated with a dextran derivative (Endorem, Revovist) [250]. Surface coating and size affect the efficiency of the magnetic nanoparticles [251]. The relaxation rates increase with the size of the nanoparticles, and the thickness coating decreases the relaxivity [252,253]. The magnetism can be modified by adding doping atoms; Fe^{2+} is replaced by transition metals as Mn^{2+}, Ni^{2+}, or Co^{2+} [254].

An example of theranostic nanoparticles is mesoporous silica matrix loaded with magnetic iron oxide nanoobjects and drugs and having a phosphonate coating; these nanosystems can cross the cellular membrane and can be internalized by pancreatic cancer cells. The use of an external magnetic field allows to control the locations of the nanoparticles [255].

Treatment of cancer via hyperthermia by tissue heating at 42–45°C, in conjunction with radiation and chemotherapy, has resulted in synergistic effects to increase the efficacy of conventional treatments and has allowed to reduce toxic side effects [256]. In magnetically mediated hyperthermia (MMH), the heating of tissue is generated by magnetic nanoparticles in the presence of an alternating magnetic field (AMF) [257]. Iron oxide nanoparticles are able to passively and actively target tumors and, upon activation by an external alternating magnetic field, generate heat via multiple possible loss mechanisms: hysteresis, Néel paramagnetic switching, and friction from Brownian rotation [258]. Grafting the nanoparticle surface with active targeting ligands has shown an improve tumor targeting and retention of the magnetic nanoparticles [259–261].

Magnetic nanoparticles with unique physicochemical properties have been used in a wide range of applications [262–266]. Clinical applications include imaging of the liver, gastrointestinal tract, metastatic lymph nodes, atherosclerosis, kidney diseases, and brain tumors [254,267–269].

Surface functionalized nanoparticles are used for in vivo imaging or cell labeling. Surface modification of the magnetic core with polyethylene glycol (PEG) makes the nanoparticles useful for biological systems with high colloidal stability [270,271]. Moreover, versatile surface functionalization with antibodies [272], aptamers [273], peptides [274], and small molecules [275] allows to target different receptors overexpressed on cells. These nanoparticles can be followed by multimodal imaging and also be used for therapy. Among the many types of magnetic nanoparticles, superparamagnetic iron oxides are the most used in MRI.

Yang et al. prepared iron oxide nanoparticles coated with HER2/neu antibody conjugated poly(amino acid) derivatives (PAION-Ab) for molecular MR imaging of breast cancer SKBR-3 cells (Fig. 1.8) [276]. The biocompatible poly(amino acid)-coated iron oxide nanoparticles showed no cytotoxicity. The antibody was grafted via glutaraldehyde cross-linking, and the hydrodynamic size of the antibody-grafted nanoparticles was about 31 nm. The T_2 relaxivity was 246 $mM^{-1}\ s^{-1}$ greater than that of the commercial products. T_2-weighted images of SKBR-3 breast cancer cells that overexpressed HER2/neu receptors showed enhanced signal intensities (Fig. 1.9).

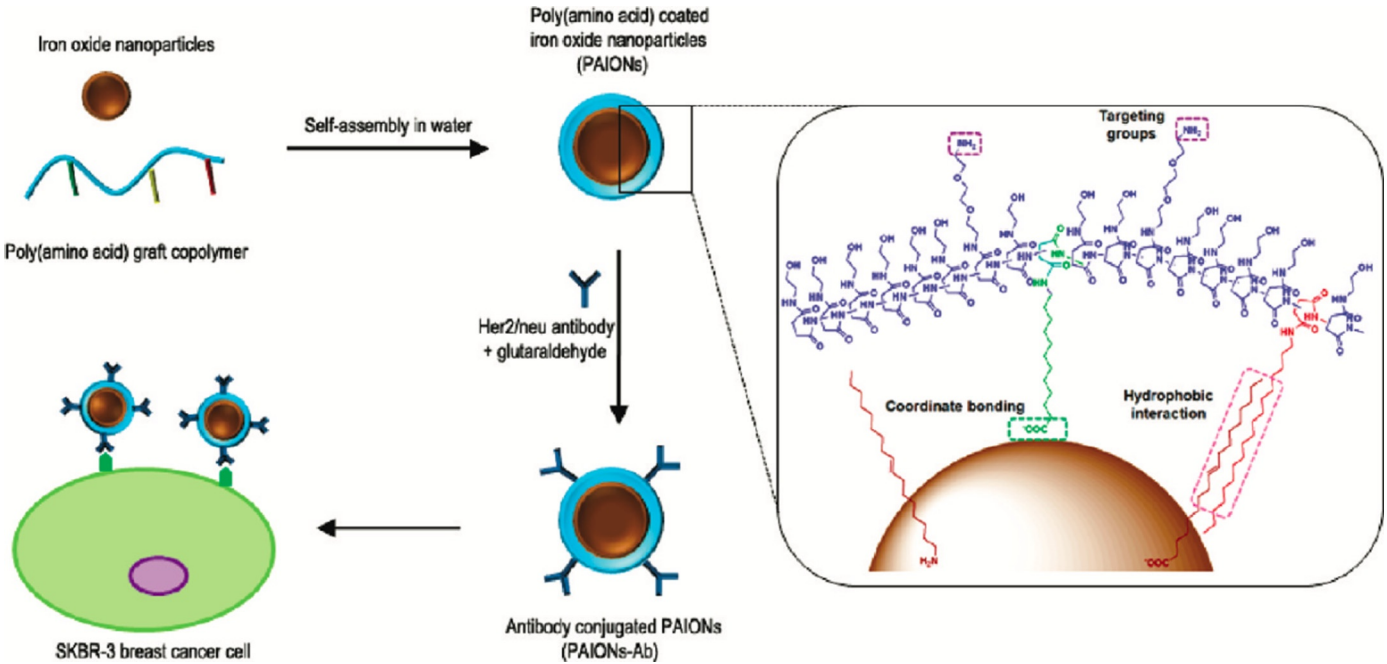

Fig. 1.8 HER2/neu antibody conjugated poly(amino acid)-coated iron oxide nanoparticles for breast cancer cell imaging. *Reprinted with permission from H.-M. Yang, C. Woo Park, M.-A. Woo, M. Il Kim, Y. Min Jo, H. Gyu Park, J.-D. Kim, HER2/neu antibody conjugated poly(amino acid)-coated iron oxide nanoparticles for breast cancer MR imaging, Biomacromolecules 11 (2010) 2866–2872. Copyright 2010, American Chemical Society.*

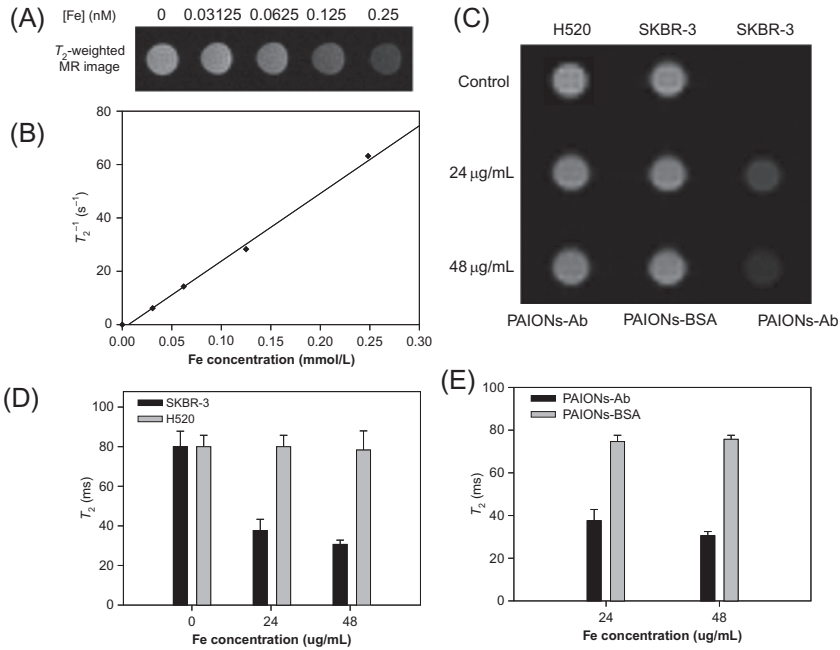

Fig. 1.9 T_2-weighted MR images of various concentrations of nanoparticles in aqueous solution at 4.7 T (A), graphs of R_2 versus the iron concentration (B), T_2-weighted MR images of SKBR-3 breast cancer cells and H520 lung cancer cells treated with PAION-Ab and PAION-BSA (C), T_2 relaxation time of SKBR-3 breast cancer cells and H520 lung cancer cells treated with PAION-Ab (D), and T_2 relaxation time of SKBR-3 breast cancer cell treated with PAION-Ab and PAION-BSA (E). *Reprinted with permission from H.-M. Yang, C. Woo Park, M.-A. Woo, M. Il Kim, Y. Min Jo, H. Gyu Park, J.-D. Kim, HER2/neu antibody conjugated poly(amino acid)-coated iron oxide nanoparticles for breast cancer MR imaging, Biomacromolecules 11 (2010) 2866–2872. Copyright 2010, American Chemical Society.*

1.4.2 Antibacterial Properties

Effective inhibition against a wide range of bacteria is well known for several nanosystems, for example, Fe_3O_4, TiO_2, CuO, and ZnO. These oxides possess greater durability, lower toxicity, and higher stability and selectivity in comparison with classical organic antibacterial agents. Nanoparticles with a diameter less than 20 nm are generally more efficient than larger one. In fact, small nanoparticles can penetrate into bacterial cells and may release toxic metal ions upon dissolution [277].

Metal oxide nanoparticles with varying physicochemical characteristics can exhibit different antibacterial mechanisms and effects. Oxide nanoparticles with a combination of two or three metals can be developed for

Table 1.3 Some examples of mixed metal oxide nanoparticles tested for their antibacterial activity [278]

Metal oxide nanoparticle	Bacterial strain tested	References
Zn/Fe oxide	*Staphylococcus aureus*, *Escherichia coli*	[279]
Zn/Mg oxide	*E. coli*, *Bacillus subtilis*	[280]
ZnO/Au	*E. coli*, *S. aureus*	[281]
TiO_2/Ag	*S. aureus*	[282]
Fe_3O_4/Ag	*S. aureus*	[283]

efficient elimination of various bacterial strains, even those highly resistant to traditional treatments (Table 1.3) [278].

Guo et al. [284] have reported that when ZnO nanoparticles are doped with Ta, their bactericidal activity is higher than that of pure nano-ZnO systems.

In another study, He et al. [281] have observed that deposition of small Au particles (3 nm of diameter) onto the surface of ZnO nanoparticles, even at a very low ZnO/Au molar ratio (0.2%), significantly enhanced the photocatalytic and antibacterial activity of ZnO nanoobjects.

Different studies suggested that the most important factor that determines the toxicity of metal oxide nanoparticles is the inherent toxicity of the metal ions released [285] and the induction of reactive oxygen species (ROS) generation [286].

Li et al. studied the ROS production kinetics of seven metal oxide nanoparticles (TiO_2, ZnO, Al_2O_3, $nSiO_2$, Fe_2O_3, CeO_2, and CuO) under UV irradiation (365 nm) [287]. The results showed that different metal oxides had distinct photogenerated ROS kinetics. TiO_2 and ZnO nanoparticles generated three types of ROS (superoxide radical, hydroxyl radical, and singlet oxygen), whereas other metal oxides generated only one or two types or did not generate any type of ROS (Fig. 1.10). The ROS generation mechanism was investigated by comparing the electronic structures of the metal oxides with the redox potentials of various ROS generation. To develop a quantitative relationship between oxidative stress and antibacterial activity of NPs, they examined the viability of E. coli cells in aqueous suspensions of NPs under UV irradiation, and a linear correlation was found between the average concentration of total ROS and the bacterial survival rates.

1.4.3 Biomedical Implant

Bioceramics are important in the biomedical field and are ideal for surgical implants thanks to their thermal and chemical inertness. They have high

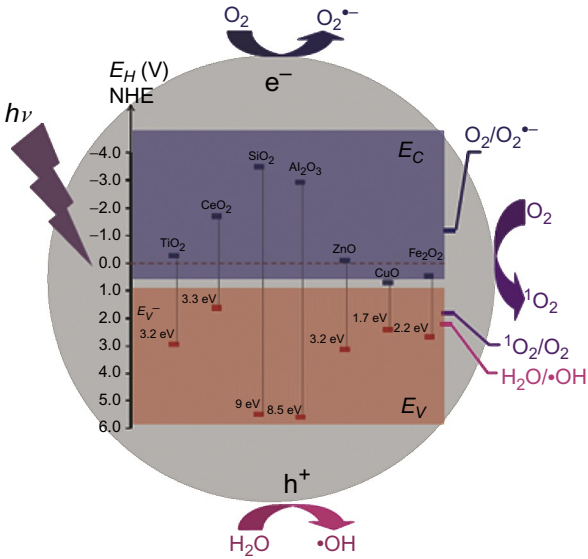

Fig. 1.10 Principle of photogenerated reactive oxygen species. *Reprinted with permission from Y. Li, W. Zhang, J. Niu, Y. Chen, Mechanism of photogenerated reactive oxygen species and correlation with the antibacterial properties of engineered metal-oxide nanoparticles, ACS Nano 6(6) (2012) 5164–5173. Copyright 2012, American Chemical Society.*

strength, wear resistance, and durability. They can also stimulate bone growth and have low friction coefficients. They do not create strong biologically relevant interfaces with bones, but they do promote strong adhesions to bones [288]. Joint/tissue replacement, metal coating to increase biocompatibility, or resorbable lattice to provide a structure that can be replaced by the body tissues are the most principal applications of ceramic biomaterials.

Bioceramics are not exclusively resorbable; they can also be bioactive, biodegradable, and soluble and are also available as composites with a polymer component and microspheres [289].

Alumina (Al_2O_3) and zirconia (ZrO_2) are the most used metal oxides for biomedical implant. Alumina is highly inert, even under physiological conditions and has excellent wear resistance and hardness. It is used for dental applications and functions as vertebrae spacers and extensors [289,290]. The body normally reacts to alumina by forming nonadherent fibers around the implant [289]. Zirconia is also inert under physiological conditions. Partially stabilized zirconia (PSZ) has a higher flexural strength, toughness,

and reliability and lower Young's modulus. Zirconia is good for long-term clinical uses [289]. It is widely used in total hip replacement and as a replacement for knees, tendons, ligaments, and teeth [290]. Zirconia-based bioceramics include yttria-stabilized tetragonal polycrystalline zirconia (Y-TZP) and zirconia/alumina composites [287,289], but different systems, as ceria- and magnesia-doped zirconia (Ce-TZP and Mg-PSZ), had also been introduced. If Y-TZP is preferred for orthopedic implants due to its high strength. Ce-TZP and Mg-PSZ are competitive with Y-TZP in toughness and strength.

Tantalum has excellent anticorrosion and biocompatibility properties. Tantalum oxide (Ta_2O_5) nanotube films can be produced on tantalum by controlling the conditions of anodization and annealing. Wang et al. investigated the influence of Ta_2O_5 nanotube films on pure tantalum (Fig. 1.11) [291]. The results showed that Ta_2O_5 nanotube films have high

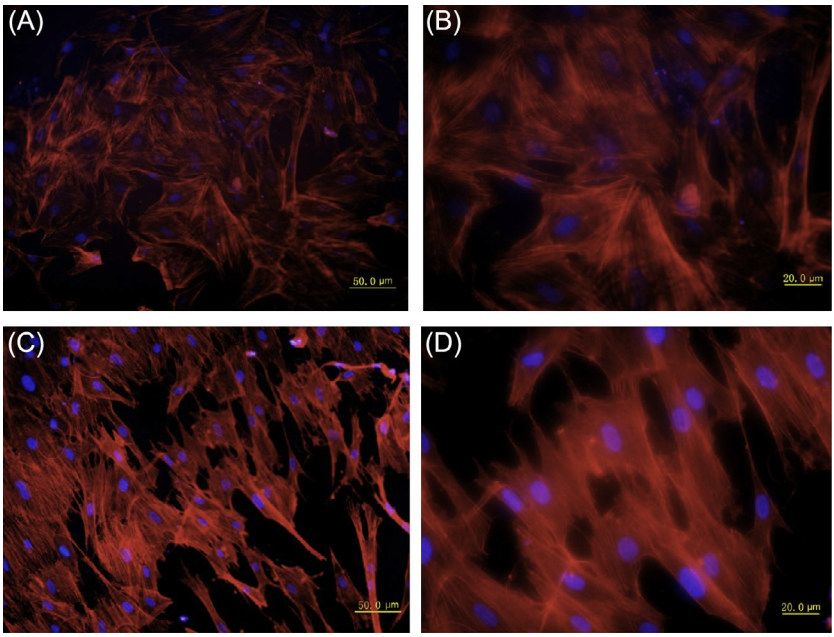

Fig. 1.11 Fluorochrome micrography of rBMSCs after incubation for 48 h. rBMSCs on the nanotube surface (panels C and D) have a more regular arrangement of the actin cytoskeleton and more obviously have a polygonal and elongated form than on the untreated tantalum surface (panels A and B). *Reprinted with permission from Y. Li, W. Zhang, J. Niu, Y. Chen, Mechanism of photogenerated reactive oxygen species and correlation with the antibacterial properties of engineered metal-oxide nanoparticles, ACS Nano 6(6) (2012) 5164–5173. Copyright 2012, American Chemical Society.*

anticorrosion capability and can increase the protein adsorption to tantalum and promote the adhesion, proliferation, and differentiation of rabbit bone mesenchymal stem cells (rBMSCs) and the mRNA expression of osteogenic gene such as Osterix, ALP, collagen-I, and osteocalcin on tantalum. Ta_2O_5 nanotube films can improve the anticorrosion, biocompatibility, and osteoinduction of pure tantalum, which provides the theoretical elaboration for development of tantalum endosseous implant or implant coating to a certain extent.

REFERENCES

[1] Z. Feng, W.T. Hong, D.D. Fong, Y.L. Lee, Y. Yacoby, D. Morgan, Y. Shao-Horn, Catalytic activity and stability of oxides: the role of near-surface atomic structures and compositions, Acc. Chem. Res. 49 (5) (2016) 966–973.

[2] S. Gupta, W. Kellogg, H. Xu, X. Liu, J. Cho, G. Wu, Bifunctional perovskite oxide catalysts for oxygen reduction and evolution in alkaline media, Chem. Asian J. 11 (1) (2016) 10–21.

[3] Y.F. Sun, S.B. Liu, F.L. Meng, J.Y. Liu, Z. Jin, L.T. Kong, J.H. Liu, Metal oxide nanostructures and their gas sensing properties: a review, Sensors (Basel) 12 (3) (2012) 2610–2631.

[4] E. Fortunato, P. Barquinha, R. Martins, Oxide semiconductor thin-film transistors: a review of recent advances, Adv. Mater. 24 (22) (2012) 2945–2986.

[5] Y. Zhang, X. Yan, Y. Yang, Y. Huang, Q. Liao, J. Qi, Scanning probe study on the piezotronic effect in ZnO nanomaterials and nanodevices, Adv. Mater. 24 (34) (2012) 4647–4655.

[6] X. Yu, T.J. Marks, A. Facchetti, Metal oxides for optoelectronic applications, Nat. Mater. 15 (4) (2016) 383–396.

[7] B.L. Ellis, P. Knauth, T. Djenizian, Three-dimensional self-supported metal oxides for advanced energy storage, Adv. Mater. 26 (21) (2014) 3368–3397.

[8] Z. Chen, C.H. Shek, C.M. Wu, J.K. Lai, Characterization strategies for Mn_2O_3 nanomaterials, J. Nanosci. Nanotechnol. 14 (2) (2014) 1693–1709.

[9] A. Dhillon, M. Nair, S.K. Bhargava, D. Kumar, Excellent fluoride decontamination and antibacterial efficacy of Fe-Ca-Zr hybrid metal oxide nanomaterial, J. Colloid Interface Sci. 457 (2015) 289–297.

[10] J. Si, J. Zhang, S. Liu, W. Zhang, D. Yu, X. Wang, L. Guo, S.G. Shen, Characterization of a micro-roughened TiO_2/ZrO_2 coating: mechanical properties and HBMSC responses in vitro, Acta Biochim. Biophys. Sin. Shanghai 46 (7) (2014) 572–581.

[11] Y. Li, A. Coughlan, A.W. Wren, Investigating the surface reactivity of SiO_2-TiO_2-CaO-Na_2O/SrO bioceramics as a function of structure and incubation time in simulated body fluid, J. Mater. Sci. Mater. Med. 25 (8) (2014) 1853–1864.

[12] S.M. Naga, A.M. El-Kady, H.F. El-Maghraby, M. Awaad, R. Detsch, A. R. Boccaccini, Novel porous Al_2O_3-SiO_2-TiO_2 bone grafting materials: formation and characterization, J. Biomater. Appl. 28 (6) (2014) 813–824.

[13] Z. Karimi, L. Karimi, H. Shokrollahi, Nano-magnetic particles used in biomedicine: core and coating materials, Mater. Sci. Eng. C Mater. Biol. Appl. 33 (5) (2013) 2465–2475.

[14] N. Casañ-Pastor, P. Gómez-Romero, Polyoxometalates: from inorganic chemistry to materials science, Front. Biosci. 9 (2004) 1759–1770.

[15] P. Bollella, G. Fusco, C. Tortolini, G. Sanzò, G. Favero, L. Gorton, R. Antiochia, Beyond graphene: electrochemical sensors and biosensors for biomarkers detection, Biosens. Bioelectron. S0956-5663 (16) (2016) 30267–30276.
[16] S. Teich, W. Al-Rawi, M. Heima, F.F. Faddoul, G. Goldzweig, Z. Gutmacher, D. Aizenbud, Image quality evaluation of eight complementary metal-oxide semiconductor intraoral digital X-ray sensors, Int. Dent. J. (2016), https://doi.org/10.1111/idj.12241.
[17] J. Fierro, Metal Oxides: Chemistry and Applications, CRC Press/Taylor and Francis Group, London, 2006.
[18] S. Bagheri, N. Muhd Julkapli, S. Bee Abd Hamid, Titanium dioxide as a catalyst support in heterogeneous catalysis, Sci. World J. 2014 (2014) 727496.
[19] T.A. Egerton, UV-absorption—the primary process in photocatalysis and some practical consequences, Molecules 9 (11) (2014) 18192–18214.
[20] M. Labanowska, EPR monitoring of redox processes in transition metal oxide catalysts, ChemPhysChem 2 (12) (2001) 712–731.
[21] Y. Liu, D. Tu, H. Zhu, X. Chen, Lanthanide-doped luminescent nanoprobes: controlled synthesis, optical spectroscopy, and bioapplications, Chem. Soc. Rev. 42 (16) (2013) 6924–6958.
[22] S. Uthaman, S.J. Lee, K. Cherukula, C.S. Cho, I.K. Park, Polysaccharide-coated magnetic nanoparticles for imaging and gene therapy, Biomed. Res. Int. 2015 (2015) 95917.
[23] E. Comini, Integration of metal oxide nanowires in flexible gas sensing devices, Sensors (Basel) 13 (8) (2013) 10659–10673.
[24] M.S. Draz, B.A. Fang, P. Zhang, Z. Hu, S. Gu, K.C. Weng, J.W. Gray, F.F. Chen, Nanoparticle-mediated systemic delivery of siRNA for treatment of cancers and viral infections, Theranostics 4 (9) (2014) 872–892.
[25] J.I. Hahm, Biomedical detection via macro- and nano-sensors fabricated with metallic and semiconducting oxides, J. Biomed. Nanotechnol. 9 (1) (2013) 1–25.
[26] R.E. Yanes, F. Tamanoi, Development of mesoporous silica nanomaterials as a vehicle for anticancer drug delivery, Ther. Deliv. 3 (3) (2012) 389–404.
[27] D.A. Riccio, M.H. Schoenfisch, Nitric oxide release: part I. Macromolecular scaffolds, Chem. Soc. Rev. 41 (10) (2012) 3731–3741.
[28] A. Gurav, T. Kodas, T. Pluym, Y. Xiong, Aerosol processing of materials, Aerosol Sci. Technol. 19 (1993) 411–452.
[29] F.E. Kruis, H. Fissan, A. Peled, Synthesis of nanoparticles in the gas phase for electronic, optical and magnetic applications: a review, J. Aerosol Sci. 29 (1998) 511–535.
[30] R. Strobel, S.E. Pratsinis, Flame aerosol synthesis of smart nanostructured materials, J. Mater. Chem. 17 (2007) 4743–4756.
[31] B.L. Cushing, V.L. Kolesnichenko, C.J. O'Connor, Recent advances in the liquid-phase syntheses of inorganic nanoparticles, Chem. Rev. 104 (2004) 3893–3946.
[32] J. Hou, C. Yang, Z. Wang, W. Zhou, S. Jiao, H. Zhu, *In situ* synthesis of α-β phase heterojunction on Bi_2O_3 nanowires with exceptional visible-light photocatalytic performance, Appl. Catal. B Environ. 142–143 (2013) 504–511.
[33] Y. Cao, F. Yuan, M. Yao, J.H. Bang, J.H. Lee, A new synthetic route to hollow Co_3O_4 octahedra for supercapacitor applications, CrstEngComm 16 (2014) 826–833.
[34] D. Su, X. Xie, P. Munroe, S. Dou, G. Wang, Mesoporous hexagonal Co_3O_4 for high performance lithium ion batteries, Sci. Rep. 4 (2014), https://doi.org/10.1038/srep06519.
[35] O. Rubilar, M. Rai, G. Tortella, M.C. Diez, A.B. Seabra, N. Durá, Biogenic nanoparticles: copper, copper oxides, copper sulfides, complex copper nanostructures and their applications, Biotechnol. Lett. 35 (2013) 1365–1375.
[36] P. Kanhed, S. Birla, S. Gaikwad, A. Gade, A.B. Seabra, O. Rubilar, N. Duran, M. Rai, *In vitro* antifungal efficacy of copper nanoparticles against selected crop pathogenic fungi, Mater. Lett. 115 (2014) 13–17.

[37] P.S. Haddad, A.B. Seabra, Biomedical applications of magnetic nanoparticles, in: A. I. Martinez (Ed.), Iron Oxides: Structure, Properties and Applications, vol. 1, Nova Science Publishers, Inc., New York, NY, 2012, pp. 165–188.
[38] A.B. Seabra, T. Pasquoto, A.C.F. Ferrarini, M. Cruz, P.S. Haddad, R. de Lima, Preparation, characterization, cytotoxicity and genotoxicity evaluations of thiolated- and *S*-nitrosated superparamagnetic iron oxide nanoparticles: implications for cancer treatment, Chem. Res. Toxicol. 27 (2014) 1207–1218.
[39] M.M. Molina, A.B. Seabra, M.G. de Oliveira, R. Itri, P.S. Haddad, Nitric oxide donor superparamagnetic iron oxide nanoparticles, Mater. Sci. Eng. C 33 (2013) 746–751.
[40] S. Laurent, D. Forge, M. Port, A. Roch, C. Robic, L. Vander Elst, R.N. Muller, Magnetic iron oxide nanoparticles: synthesis, stabilization, vectorization, physico-chemical characterizations and biological applications, Chem. Rev. 108 (6) (2008) 2064–2110.
[41] M. Vukovic, Z. Brankovic, D. Poleti, A. Recnik, G. Brankovic, Novel simple methods for the synthesis of single-phase valentinite Sb_2O_3, J. Sol-Gel Sci. Technol. 72 (2014) 527–533.
[42] Y.Y. Zhu, L.M. Liao, Applications of nanoparticles for anticancer drug delivery: a review, J. Nanosci. Nanotechnol. 7 (2015) 4753–4773.
[43] A.B. Seabra, N. Duran, Nitric oxide-releasing vehicles for biomedical applications, J. Mater. Chem. 20 (2010) 1637–1664.
[44] A.A. Keller, S. McFerran, A. Lazareva, S. Suh, Global life cycle releases of engineered nanomaterials, J. Nanopart. Res. 15 (2013) 1692.
[45] P.S. Goh, B.C. Ng, W.J. Lau, A.F. Ismail, Inorganic nanomaterials in polymeric ultrafiltration membranes for water treatment, Sep. Purif. Rev. 44 (2015) 216–249.
[46] R.W. Tarnuzzer, J. Colon, S. Patil, S. Seal, Vacancy engineered ceria nanostructures for protection from radiaton-induced cellular damage, Nano Lett. 5 (12) (2005) 2573–2577.
[47] J.P. Chen, S. Patil, S. Seal, J.F. McGinnis, Rare earth nanoparticles prevent retinal degeneration induced by intracellular peroxides, Nat. Nanotechnol. 1 (2) (2006) 142–150.
[48] D.R. Lovley, E.J.P. Phillips, Bioremediation of uranium contamination with enzymatic uranium reduction, Environ. Sci. Technol. 26 (1992) 2228–2234.
[49] D. Lovley, E.J.P. Phillips, Reduction of uranium by *Desulfovibrio desulfuricans*, Appl. Environ. Microbiol. 58 (1992) 850–856.
[50] K. Prasad, A.K. Jha, ZnO nanoparticles: synthesis and adsorption study, Nat. Sci. 1 (2009) 129–135.
[51] S. Somiya, N. Yamamoto, H. Yanagina, Science and Technology of Zirconia III (Advances in Ceramics), vols. 24A and 24B, American Ceramic Society, Westerville, OH, 1988.
[52] V. Bansal, D. Rautaray, A. Ahmad, M. Sastry, Biosynthesis of zirconia nanoparticles using the fungus *Fusarium oxysporum*, J. Mater. Chem. 14 (2004) 3303–3305.
[53] V.K. Vidhu, D. Philip, Biogenic synthesis of SnO_2 nanoparticles: evaluation of antibacterial and antioxidant activities, Spectrochim. Acta A Mol. Biomol. Spectrosc. 134 (2015) 372–379.
[54] M. Niederbergen, N. Pinna, Metal Oxide Nanoparticles in Organic Solvents: Synthesis, Formation, Assembly and Applications, Springer, London, 2009.
[55] C.T. Campbell, C.H. Peden, Chemistry. Oxygen vacancies and catalysis on ceria surfaces, Science 309 (5735) (2005) 713–714.
[56] G.A. Silva, Neuroscience nanotechnology: process, opportunities and challenges, Nat. Rev. Neurosci. 7 (1) (2006) 65–74.
[57] A.H. Faraji, P. Wipf, Nanoparticles in cellular drug delivery, Bioorg. Med. Chem. 7 (8) (2009) 2950–2962.

[58] H.T. Song, J.S. Choi, Y.M. Huh, S. Kim, Y.W. Jun, J.S. Suh, J. Cheon, Surface modulation of magnetic nanocrystals in the development of highly efficient magnetic resonance probes for intracellular labeling, J. Am. Chem. Soc. 127 (28) (2005) 9992–9993.
[59] W.H. Suh, K.S. Suslick, G.D. Stucky, Y.H. Suh, Nanotechnology, nanotoxicology and neuroscience, Prog. Neurobiol. 87 (3) (2009) 133–170.
[60] N.L. Rosi, C.A. Mirkin, Nanostructures in biodiagnostics, Chem. Rev. 105 (4) (2005) 1547–1562.
[61] D.B. Haddow, J.M. Kelly, P.F. James, R.D. Short, A.M. Scutt, R. Rawsterne, S. Kothari, Cell response to sol-gel derived titania coatings, J. Mater. Chem. 10 (12) (2000) 2795–2801.
[62] S.E. Kim, J.H. Lim, S.C. Lee, S.C. Nam, H.G. Kang, J. Choi, Anodically nanostructured titanium oxides for implant applications, Electrochim. Acta 53 (14) (2008) 4846–4851.
[63] K. Hola, Z. Markova, G. Zoppellaro, J. Tucek, R. Zboril, Tailored functionalization of iron oxide nanoparticles for MRI, drug delivery, magnetic separation and immobilization of biosubstances, Biotechnol. Adv. 33 (6 Pt 2) (2015) 1162–1176.
[64] E. Amstad, M. Textor, E. Reimhult, Stabilization and functionalization of iron oxide nanoparticles for biomedical applications, Nanoscale 3 (7) (2011) 2819–2843.
[65] C. Korsvik, S. Patil, S. Seal, W.T. Self, Superoxide dismutase mimetic properties exhibited by vacancy engineered ceria nanoparticles, Chem. Commun. 10 (2007) 1056–1058.
[66] A.S. Karakoti, N.A. Monteiro-Riviere, R. Aggarwal, J.P. Davis, R.J. Narayan, W.T. Self, J. McGinnis, S. Seal, Nanoceria as antioxidant: synthesis and biomedical applications, JOM 60 (3) (2008) 33–37.
[67] E.G. Heckert, A.S. Karakoti, S. Seal, W.T. Self, The role of cerium redox state in the SOD mimetic activity of nanoceria, Biomaterials 29 (18) (2008) 2705–2709.
[68] T.D. Scladt, T. Fraf, W. Tremel, Synthesis and characterization of monodisperse manganese oxide nanoparticles—evaluation of the nucleation and growth mechanism, Chem. Mater. 21 (14) (2009) 3183–3190.
[69] T.D. Nguyen, T.O. Do, General two-phase routes to synthesize colloid metal oxide nanocrystals, simple synthesis and ordered self-assembly structures, J. Phys. Chem. C 113 (26) (2009) 11204–112014.
[70] N.V. Long, C.M. Thi, Y. Yong, Y. Cao, H. Wu, M. Nogami, Synthesis and characterization of Fe-based metal and oxide based nanoparticles: discoveries and research highlights of potential applications in biology and medicine, Recent Pat. Nanotechnol. 8 (1) (2014) 52–61.
[71] Q.C. Zhang, Z.H. Yu, G. Li, Q.M. Ye, L.H. Lin, Synthesis of quantum-size cerium oxide nanocrystallines by a novel homogeneous precipitation method, J. Alloys Compd. 477 (1–2) (2009) 81–84.
[72] Q.L. Zhang, Z.M. Yang, B.J. Ding, Synthesis of cerium oxide nanoparticles by the precipitation method, Mater. Res. 610–613 (2009) 233–238.
[73] A.I.Y. Tok, S.W. Du, F.Y.C. Boey, W.K. Chong, Hydrothermal synthesis and characterization of rare earth doped ceria nanoparticles, Mater. Sci. Eng. A Struct. Mater. Proper. Microstruct. Process. 466 (1–2) (2007) 223–229.
[74] H.I. Chen, H.Y. Chang, Synthesis of nanocrystalline cerium oxide particles by the precipitation method, Ceram. Int. 31 (6) (2005) 795–802.
[75] Y. Yin, A.P. Alivisatos, Colloidal nanocrystal synthesis and the organic-inorganic interface, Nature 437 (7059) (2005) 664–670.
[76] N.A.S. Amin, E. Matijevic, Magnetic properties of uniform spherical magnetite particles prepared from ferrous hydroxide gels, Phys. Status Solidi A 101 (1987) 233–238.

[77] M.M.E. Ozaki, Preparation and magnetic properties of monodispersed spindle-type g-Fe_2O_3 particles, J. Colloid Interface Sci. 107 (1) (1985) 199–203.
[78] A. Walters, C. Billotey, A. Garofalo, C. Ulhaq-Bouillet, C. Lefèvre, J. Taleb, S. Laurent, L. Vander Elst, R.N. Muller, L. Lartigue, F. Gazeau, D. Felder-Flesch, S. Begin-Colin, Mastering shape and composition of dendronized iron oxide nanoparticles to tailor magnetic resonance imaging and hyperthermia, Chem. Mater. 26 (18) (2014) 5252–5264.
[79] J.H. Gao, H.W. Gu, B. Xu, Multifunctional magnetic nanoparticles: design, synthesis and biomedical applications, Acc. Chem. Res. 42 (8) (2009) 1097–1107.
[80] A.K. Madl, K.E. Pinkerton, Health effects of inhaled engineered and incidental nanoparticles, Crit. Rev. Toxicol. 39 (8) (2009) 629–658.
[81] V. Stone, H. Johnston, R.P.F. Schins, Development of in vitro systems for nanotoxicology: methodological considerations, Crit. Rev. Toxicol. 39 (7) (2009) 613–626.
[82] M.V.D.Z. Park, D.P.K. Lankveld, H. van Loveren, W.H. De jong, The status of in vitro toxicity studies in the risk assessment of nanomaterials, Nanomedicine 4 (6) (2009) 669–685.
[83] H. Meng, T. Xia, S. George, A.E. Nel, A predictive toxicological paradigm for the safety assessment of nanomaterials, ACS Nano 3 (7) (2009) 1620–1627.
[84] C.F. Jones, D.W. Grainger, In vitro assessments of nanomaterial toxicity, Adv. Drug Deliv. Rev. 61 (6) (2009) 438–456.
[85] R. Hardman, A toxicologic review of quantum dots: toxicity depends on physicochemical and environmental factors, Environ. Health Perspect. 114 (2) (2006) 165–172.
[86] R. Sequeira, A. Genaidy, G. Weckman, R. Shell, W. Karwowski, A. Acosta-Leon, Health effects of nanomaterials: a critical approach and research to practice, Hum. Factors Ergon. Manuf. 18 (3) (2008) 293–341.
[87] R. Landsiedel, M.D. Kapp, M. Schulz, K. Wiench, F. Oesch, Genotoxicity investigations on nanomaterials: methods, preparation and characterization of test material, potential artifacts and limitations—many questions, some answers, Mutat. Res. Rev. Mutat. Res. 681 (2–3) (2009) 241–258.
[88] B. Fahmy, S.A. Cormier, Copper oxide nanoparticles induce oxidative stress and cytotoxicity in airway epithelial cells, Toxicol. In Vitro 23 (7) (2009) 1365–1371.
[89] L.K. Limbach, Y.C. Li, R.N. Grass, T.J. Brunner, M.A. Hintermann, M. Muller, D. Gunther, W.J. Stark, Oxide nanoparticle uptake in human lung fibroblasts: effects of particle size, agglomeration and diffusion at low concentrations, Environ. Sci. Technol. 39 (23) (2005) 9370–9376.
[90] Y.Q. Ge, Y. Zhang, J.G. Xia, M. Ma, S.Y. He, F. Nie, N. Gu, Effect of surface charge and agglomerate degree of magnetic iron oxide nanoparticles on KB cellular uptake in vitro, Colloids Surf. B Biointerfaces 73 (2) (2009) 294–301.
[91] A.S. Karakoti, L.L. Hench, S. Seal, The potential toxicity of nanomaterials – the role of surface, JOM 58 (7) (2006) 77–82.
[92] T. Cedervall, I. Lynch, S. Lindman, T. Berggard, E. Thulin, H. Nilsson, K.A. Dawson, S. Linse, Understanding the nanoparticle-protein corona using methods to quantify exchange rates and affinities of proteins for nanoparticles, Proc. Natl. Acad. Sci. U. S. A. 104 (7) (2007) 2050–2055.
[93] P. Aggarwal, J.B. Hall, C.B. McLeland, M.A. Dobrovolskaia, S.E. MCNeil, Nanoparticle interaction with plasma proteins as it relates to particle biodistribution, biocompatibility and therapeutic efficiency, Adv. Drug Deliv. Rev. 61 (6) (2009) 428–437.
[94] M. Mahmoudi, S.N. Saeedi-Eslami, M.A. Shokrgozar, K. Azadmanesh, M. Hasanloo, H. Kalhor, C. Burtea, B. Rothen-Rutishauser, S. Laurent, S. Sheibani, H. Vali, Cell

"vision": complementary factor of protein corona in nanotoxicology, Nanoscale 4 (17) (2012) 5461–5468.
[95] Z.J. Deng, G. Mortimer, T. Schiller, A. Musmeci, D. Martin, R.F. Minchin, Differential plasma protein binding to metal oxide nanoparticles, Nanotechnology 20 (45) (2009) 455101.
[96] H. Kung, Transition metal oxides, Surface Chemistry and Catalysis, first ed., Elsevier Science, Amsterdam, The Netherlands, 1989.
[97] T. Takada, N. Yamamoto, T. Shinjo, M. Kiyama, Y. Bando, Magnetic properties of a-Fe_2O_3 fine particles, Bull. Inst. Chem. Res. 43 (4–5) (1966) 406–415.
[98] T. Moriya, T. Takimoto, Anomalous properties around magnetic instability in heavy electron systems, J. Phys. Soc. Jpn. 64 (1995) 960–969.
[99] Y. Bando, M. Kiyama, N. Yamamoto, T. Takada, T. Shinjo, H. Takaki, The magnetic properties of α-Fe_2O_3 fine particles, J. Phys. Soc. Jpn. 20 (1965) 2086–2089.
[100] G.J. Muench, S. Arajs, E. Matijevic, Magnetic properties of monodispersed submicromic α-Fe_2O_3 particles, J. Appl. Phys. 52 (1981) 2493–2495.
[101] W.J. Schuclc, V.D. Deetsneek, Appearance of a weak ferromagnetism in fine particles of antiferromagnetic materials, J. Appl. Phys. 33 (1962) 1136–1140.
[102] N. Yamamoto, The shift of the spin flip temperature α-Fe_2O_3 nanoparticles, J. Phys. Soc. Jpn. 24 (1968) 23–28.
[103] C.R. Vestal, Z.J. Zhang, Effects of surface coordination chemistry on the magnetic properties of MnFe(2)O(4) spinel ferrite nanoparticles, J. Am. Chem. Soc. 125 (22) (2003) 9828–9833.
[104] A. Zhukov, A.F. Cobeno, J. Gonzalez, J.M. Blanco, P. Aragoneses, L. Dominguez, Magnetoelastic sensor of liquid level based on magnetoelastic properties of Co-rich microwires, Sens. Actuators A Phys. 81 (2000) 129–133.
[105] S.D. Bhame, Tuning of the magnetostrictive properties of $CoFe_2O_4$ by Mn substitution for Co, J. Appl. Phys. 100 (2006) 113911.
[106] I.-B. Kim, M.H. Han, R.L. Phillips, B. Samanta, V.M. Rotello, Z.J. Zhang, U.H.F. Bunz, Nano-conjugate fluorescence probe for the discrimination of phosphate and pyrophosphate, Chem. A Eur. J. 15 (2009) 449–456.
[107] C. Xia, W. Ning, G. Lin, Facile synthesis of novel MnO_2 hierarchical nanostructures and their application to nitrite sensing, Sens. Actuators B Chem. 137 (2009) 710–714.
[108] G. Wang, F. Meng, C. Ding, P.K. Chu, X. Liu, Microstructure, bioactivity and osteoblast behavior of monoclinic zirconia coating with nanostructured surface, Acta Biomater. 6 (2010) 990–1000.
[109] K.E. Scarberry, E.B. Dickerson, J.F. McDonald, Z.J. Zhang, Magnetic nanoparticle-peptide conjugates for in vitro and in vivo targeting and extraction of cancer cells, J. Am. Chem. Soc. 130 (2008) 10258–10262.
[110] Y.S. Yim, J.S. Choi, G.T. Kim, C.H. Kim, T.H. Shin, D.G. Kim, J. Cheon, A facile approach for the delivery of inorganic nanoparticles into the brain by passing through the blood-brain barrier (BBB), Chem. Commun. 48 (2012) 61–63.
[111] S. Laurent, S. Boutry, I. Mahieu, L. Vander Elst, R.N. Muller, Iron oxide based MR contrast agents: from chemistry to cell labeling, Curr. Med. Chem. 16 (35) (2009) 4712–4727.
[112] X. Mou, Z. Ali, S. Li, N. He, Applications of magnetic nanoparticles in targeted drug delivery system, J. Nanosci. Nanotechnol. 15 (1) (2015) 54–62.
[113] X. Michalet, F.F. Pinaud, L.A. Bentolila, J.M. Tsay, S. Doose, J.J. Li, G. Sundaresan, A.M. Wu, S.S. Gamblir, S. Weiss, Quantum dots for live cells, in vivo imaging and diagnostics, Science 307 (2005) 538–544.
[114] H.B. Na, J.H. Lee, K. An, Y.I. Park, M. Park, I.S. Lee, D.H. Nam, S.T. Kim, S.H. Kim, K.W. Kim, K.S. Kim, S.O. Kim, T. Hyeon, Development of a T1 contrast agent for magnetic resonance imaging using MnO nanoparticles, Angew. Chem. Int. Ed. 46 (2007) 5397–5401.

[115] J. Moger, B.D. Johnston, C.R. Tyler, Imaging metal oxide nanoparticles in biological structures with CARS microscopy, Opt. Express 16 (5) (2008) 3408–3419.
[116] J. Yang, J. Gunn, S.R. Dave, M. Zhang, Y.A. Wang, X. Gao, Ultrasensitive detection and molecular imaging with magnetic nanoparticles, Analyst 133 (2) (2008) 154–160.
[117] H. Kind, H. Yan, B. Messer, M. Law, P. Yang, Nanowire ultraviolet photodetectors and optical switches, Adv. Mater. 14 (2002) 158–160.
[118] W.I. Park, G.C. Yi, Electroluminescence in n-ZnO nanorod arrays vertically grown on p-GaN, Adv. Mater. 16 (2004) 87–90.
[119] R. Könenkamp, R.C. Word, C. Schlegel, Vertical nanowire light-emitting diode, Appl. Phys. Lett. 85 (2004) 6004–6006.
[120] K. Keem, H. Kim, G.T. Kim, J.S. Lee, Photocurrent in ZnO nanowires grown from Au electrodes, Appl. Phys. Lett. 84 (2004) 4376–4379.
[121] M.S. Arnold, P. Avouris, Z.W. Pan, Z.L. Wang, Field-effect transistors based on single semiconducting oxide nanobelts, J. Phys. Chem. B 107 (2003) 659–663.
[122] H.T. Wang, B.S. Kang, F. Ren, L.C. Tien, P.W. Sadik, D.P. Norton, S.J. Pearton, J. Lin, Hydrogen-selective sensing at room temperature with ZnO nanorods, Appl. Phys. Lett. 86 (2005) 243503.
[123] J. Zhou, N.S. Xu, S.Z. Deng, J. Chen, J.C. She, Z.L. Wang, Large-area nanowire arrays of molybdenum and molybdenum oxides: synthesis and field emission properties, Adv. Mater. 15 (2003) 1835–1840.
[124] Y. Ohhata, F. Shinoki, S. Yoshida, Optical properties of r.f. reactive sputtered tin-doped In_2O_3 films, Thin Solid Films 59 (1979) 255–261.
[125] C. Liang, G. Meng, Y. Lei, F. Phillipp, L. Zhang, Catalytic growth of semiconducting In_2O_3 nanofibers, Adv. Mater. 13 (2001) 1330–1333.
[126] M.J. Zheng, L.D. Zhang, G.H. Li, X.Y. Zhang, X.F. Wang, Ordered indium-oxide nanowire arrays and their photoluminescence properties, Appl. Phys. Lett. 79 (2001) 839–842.
[127] H. Cao, X. Qiu, Y. Liang, Q. Zhu, M. Zhao, Room-temperature ultraviolet-emitting In_2O_3 nanowires, Appl. Phys. Lett. 83 (2003) 761–763.
[128] X.C. Wu, J.M. Hong, Z.J. Han, Y.R. Tao, Fabrication and photoluminescence characteristics of single crystalline In_2O_3 nanowires, Chem. Phys. Lett. 373 (2003) 28–32.
[129] Q. Tang, W. Zhou, W. Zhang, S. Ou, K. Jiang, W. Yu, Y. Qian, Size-controllable growth of single crystal In $(OH)_3$ and In_2O_3 nanocubes, Cryst. Growth Des. 5 (2005) 147–150.
[130] P. Wu, Q. Li, X. Zou, W. Cheng, D. Zhang, C. Zhao, L. Chi, T. Xiao, Correlation between photoluminescence and oxygen vacancies in In_2O_3, SnO_2 and ZnO metal oxide nanostructures, J. Phys. Conf. Ser. 188 (2009) 012054.
[131] H. He, T.H. Wu, C.L. Hsin, K.M. Li, L.J. Chen, Y.L. Chueh, L.J. Chou, Z.L. Wang, Beaklike SnO_2 nanorods with strong photoluminescent and field-emission properties, Small 2 (2006) 116–120.
[132] Y.C. Her, J.-Y. Wu, Y.R. Lin, S.Y. Tsai, Low-temperature growth and blue luminescence of SnO_2 nanoblades, Appl. Phys. Lett. 89 (2006) 043115.
[133] J.Q. Hu, Y. Bando, D. Golberg, Self-catalyst growth and optical properties of novel SnO_2 fishbone-like nanoribbons, Chem. Phys. Lett. 372 (2003) 758–762.
[134] S.C. Lyu, Y. Zhang, H. Ruh, H.J. Lee, H.W. Shim, E.K. Suh, C.J. Lee, Synthesis of aligned carbon nanotubes using thermal chemical vapor deposition, Chem. Phys. Lett. 363 (2002) 134–138.
[135] M.H. Huang, Y. Wu, H. Feick, N. Tran, E. Webber, P. Yang, Adv. Mater. 13 (2001) 113 (8th China International Nanoscience and Technology Symposium (CINSTS09), J. Phys. Conf. Ser. 188 (2009) 012054).

[136] D. Banerjee, J.Y. Lao, D.Z. Wang, J.Y. Huang, Z.F. Ren, D. Steeves, B. Kimball, M. Sennett, Large-quantity free-standing ZnO nanowires, Appl. Phys. Lett. 83 (2003) 2061–2063.
[137] X. Wang, C.J. Summers, Z.L. Wang, Large-scale hexagonal-patterned growth of aligned ZnO nanorods for nano-optoelectronics and nanosensor arrays, Nano Lett. 4 (2004) 423–426.
[138] W.D. Yu, X.M. Li, X.D. Gao, Self-catalytic synthesis and photoluminescence of ZnO nanostructures on ZnO nanocrystal substrates, Appl. Phys. Lett. 84 (2004) 2658–2661.
[139] V.A.L. Roy, A.B. Djurišić, W.K. Chan, J. Gao, H.F. Lui, C. Surya, Luminescent and structural properties of ZnO nanorods prepared under different conditions, Appl. Phys. Lett. 83 (2003) 141–143.
[140] K. Vanheusden, C.H. Seager, W.L. Warren, D.R. Tallant, J.A. Voigt, Correlation between photoluminescence and oxygen vacancies in ZnO phosphors, Appl. Phys. Lett. 68 (1996) 403–406.
[141] A.B. Panda, G. Glaspell, M.S. El-Shall, Microwave synthesis and optical properties of uniform nanorods and nanoplates of rare earth oxides, J. Phys. Chem. C 111 (2007) 1861–1864.
[142] R. Si, Y.W. Zhang, H.P. Zhou, L.D. Sun, C.H. Yan, Controlled-synthesis, self-assembly behavior and surface-dependent optical properties of high quality rare earth oxide nanocrystals, Chem. Mater. 19 (2007) 18–27.
[143] H. Wang, M. Uchara, H. Nakamura, M. Miyasaki, H. Maeda, Synthesis of well-dispersed Y_2O_3:Eu nanocrystals and self-assembled nanodisks using a simple non hydrolytic route, Adv. Mater. 17 (2005) 2506–2509.
[144] J. Cao, J. Wu, Strain effects in low-dimensional transition metal oxides, Mater. Sci. Eng. R 71 (2011) 35–52.
[145] S. Ramanathan, Thin Film Metal-Oxides: Fundamentals and Applications in Electronics and Energy, Springer, New York, 2010.
[146] M. Imada, A. Fujimori, Y. Tokura, Metal-insulator transitions, Rev. Mod. Phys. 70 (4) (1998) 1039–1263.
[147] F. Chudnovskiy, S. Luryi, B. Spivak, Switching device based on first-order metal-insulator transition induced by external electric field, in: S. Luryi, J.M. Xu, A. Zaslavsky (Eds.), Future Trends in Microelectronics: The Nano Millennium, Wiley Interscience, New York, 2002, pp. 148–155.
[148] D.M. Newns, J.A. Misewich, C.C. Tsuei, A. Gupta, B.A. Scott, A. Schrott, Mott transition field effect transistor, Appl. Phys. Lett. 73 (6) (1998) 780–782.
[149] H. Wang, X. Yi, S. Chen, X. Fu, Fabrication of vanadium oxide micro-optical switches, Sens. Actuators A Phys. 122 (1) (2005) 108–112.
[150] M.J. Lee, Y. Park, D.S. Suh, E.H. Lee, S. Seo, D.C. Kim, R. Jung, B.S. Kang, S.E. Ahn, C.B. Lee, D.H. Seo, Y.K. Cha, I.K. Yoo, J.S. Kim, B.H. Park, Two series oxide resistors applicable to high speed and high density nonvolatile memory, Adv. Mater. 19 (22) (2007) 3919–3923.
[151] J. Lu, K.G. West, S.A. Wolf, Novel magnetic oxide thin films, in: S. Ramanathan (Ed.), Thin Film Metal-Oxides: Fundamentals and Applications in Electronics and Energy, Springer, New York, 2010 (Chapter 3).
[152] S.A. Wolf, D.D. Awschalom, R.A. Buhrman, J.M. Daughton, S. von Molnar, M.L. Roukes, A.Y. Chtchelkanova, D.M. Treger, Spintronics: a spin-based electronics vision for the future, Science 294 (2001) 1488–1495.
[153] M. Bibes, A. Barthelemy, Oxide spintronics, IEEE Trans. Electron Devices 54 (2007) 1003–1023.
[154] A. Brinkman, M. Huijben, M. van Zalk, J. Huijben, U. Zeitler, J.C. Maan, W.G. van der Wiel, G. Rijnders, D.H.A. Blank, H. Hilgenkamp, Magnetic effects at the interface between non-magnetic oxides, Nat. Mater. 6 (2007) 493–496.

[155] N.A. Spaldin, M. Fiebig, The renaissance of magnetoelectric multiferroics, Science 309 (2005) 391–392.
[156] W. Eerenstein, N.D. Mathur, J.F. Scott, Multiferroic and magnetoelectric materials, Nature 442 (2006) 759–765.
[157] R. Ramesh, N.A. Spaldin, Multiferroics: progress and prospects in thin films, Nat. Mater. 6 (2007) 21–29.
[158] S.W. Cheong, M. Mostovoy, Multiferroics: a magnetic twist for ferroelectricity, Nat. Mater. 6 (2007) 13–20.
[159] T. Zhao, A. Scholl, F. Zavaliche, K. Lee, M. Barry, A. Doran, M.P. Cruz, Y.H. Chu, C. Ederer, N.A. Spaldin, R.R. Das, D.M. Kim, S.H. Baek, C.B. Eom, R. Ramesh, Electrical control of antiferromagnetic domains in multiferroic $BiFeO_3$ films at room temperature, Nat. Mater. 5 (2006) 823–829.
[160] B. Sun, P. Han, W. Zhao, Y. Liu, P. Chen, White-light-controlled magnetic and ferroelectric properties in multiferroic $BiFeO_3$ square nanosheets, J. Phys. Chem. C 118 (32) (2014) 18814–18819.
[161] J. Paul, T. Nishimatsu, Y. Kawazoe, U.V. Waghmare, Ferroelectric phase transitions in ultrathin films of $BaTiO_3$, Phys. Rev. Lett. 99 (2007) 077601.
[162] T. Nishimatsu, U.V. Waghmare, Y. Kawazoe, D. Vanderbilt, Fast molecular-dynamics simulation for ferroelectric thin-film capacitors using a first-principles effective Hamiltonian, Phys. Rev. B 78 (2008) 104104.
[163] N.A. Hill, Why are there so few magnetic ferroelectrics? J. Phys. Chem. B 104 (2000) 6694–6709.
[164] X. Yu, T.J. Marks, A. Facchetti, Metal oxides for optoelectronic applications, Nat. Mater. 15 (2016) 383–396.
[165] N.T.S. Phan, C.S. Gill, J.V. Nguyen, Z.J. Zhang, C.W. Jones, Expanding the utility of one-pot multistep reaction networks through compartmentation and recovery of the catalyst, Angew. Chem. Int. Ed. 45 (2006) 2209–2212.
[166] Y. Li, D. He, Z. Cheng, C. Su, J. Li, Q. Zhu, Effect of calcium salts on isosynthesis over ZrO_2 catalysts, J. Mol. Catal. A 175 (2001) 267–275.
[167] M. Tepluchin, D.K. Pham, M. Casapu, L. Mädler, S. Kuretic, J.-D. Grunwaldt, Influence of single- and double-flame spray pyrolysis on the structure of $MnOx/\gamma\text{-}Al_2O_3$ and $FeOx/\gamma\text{-}Al_2O_3$ catalysts and their behaviour in CO removal under lean exhaust gas conditions, Cat. Sci. Technol. 5 (2015) 455–464.
[168] B. Dmuchovsky, M.C. Freerks, F.B. Zienty, Metal oxide activities in the oxidation of ethylene, J. Catal. 4 (1965) 577–580.
[169] C.J. Heyes, J.C. Irwin, H.A. Johnson, R.L. Moss, The catalytic oxidation of organic air pollutants: part 1. Single metal oxide catalysts, J. Chem. Technol. Biotechnol. 32 (1982) 1025–1033.
[170] J.G. McCarty, Y.F. Chang, V.L. Wong, E.M. Johansson, Kinetics of high temperature methane combustion by metal oxide catalysts, in: Symposium on Catalytic Combustion, San Francisco, Am. Chem. Soc.vol. 42, 1997, p. 158.
[171] S.F. Tahir, C.A. Koh, Catalytic oxidation of ethane over supported metal oxide catalysts, Chemosphere 34 (8) (1997) 1787–1793.
[172] E.M. Cordi, P.J. O'Neill, L. Falconer, Transient oxidation of volatile organic compounds on a CuO/Al_2O_3 catalyst, Appl. Catal. B 14 (1997) 23–26.
[173] P.W. Park, J.S. Ledford, The influence of the surface structure on the catalytic activity of alumina supported copper oxide catalysts oxidation of carbon monoxide and methane, Appl. Catal. B 15 (1998) 221–231.
[174] L. Peiyan, W. Min, S. Shaochun, H. Minmin, R. Jingfang, Y. Shomin, Y. Hengxiang, W. Qiwu, Development of non-noble metal catalysts for the purification of automotive exhaust gas, in: A. Crucq, A. Frennet (Eds.), Catalysis and Automotive Pollution Control, Elsevier, Amsterdam, 1987.

[175] K.M. Parida, A. Samal, Catalytic combustion of volatile organic compounds on Indian Ocean manganese nodules, Appl. Catal. A 182 (1999) 249–256.
[176] M.I. Zaki, M.A. Hasan, L. Pasupulety, N.E. Fouad, H. Knozinger, CO and CH_4 total oxidation over manganese oxide supported on ZrO_2, TIO_2, TiO_2-Al_2O_3 and SiO_2-Al_2O_3 catalysts, New J. Chem. 23 (1999) 1197–1202.
[177] Y.-W. Huang, C.-H. Wu, R.S. Aronstam, Toxicity of transition metal oxide nanoparticles: recent insights from in vitro studies, Materials 3 (2010) 4842–4859.
[178] C. Zener, Interaction between the d shells in the transition metals, Phys. Rev. 81 (4) (1951) 440–444.
[179] P.G. Tsyrulnikov, O.N. Kovalenko, L.L. Gogin, T.G. Starostina, A.S. Noskov, A.V. Kalinkin, G.N. Krukova, S.V. Tsybulya, E.N. Kudrya, A.V. Bubnov, Behavior of some deep oxidation catalysts under extreme conditions. 1. Comparison of resistance to thermal shock and SO_2 poisoning, Appl. Catal. A 167 (1998) 31–37.
[180] T. Asano, M. Tamura, Y. Nakagawa, K. Tomishige, Selective hydrodeoxygenation of 2-furancarboxylic acid to valeric acid over molybdenum-oxide-modified platinum catalyst, ACS Sustain. Chem. Eng. https://doi.org/10.1021/acssuschemeng.6b01640 (Accepted Manuscript).
[181] G. Korotcenkov, Metal oxides for solid-state gas sensors: what determines our choice? Mater. Sci. Eng. B 139 (2007) 1–23.
[182] N. Barsan, D. Koziej, U. Weimar, Metal oxide-based gas sensor research: how to? Sens. Actuators B 121 (2007) 18–35.
[183] G. Korotcenkov, The role of morphology and crystallographic structure of metal oxides in response of conductometric-type gas sensors, Mater. Sci. Eng. R 61 (2008) 1–39.
[184] M. Batzill, Surface science studies of gas sensing materials: SnO_2, Sensors 6 (2006) 1345–1366.
[185] C.O. Park, S.A. Akbar, Ceramics for chemical sensing, J. Mater. Sci. 38 (2003) 4611–4637.
[186] M. Batzill, U. Diebold, The surface and materials science of tin oxide, Prog. Surf. Sci. 79 (2005) 47–154.
[187] R. Moos, K. Sahner, M. Fleischer, U. Guth, N. Barsan, U. Weimar, Solid state gas sensor research in Germany – a status report, Sensors 9 (2009) 4323–4365.
[188] M.N. Rumyantseva, A.M. Gas'kov, Chemical modification of nanocrystalline metal oxides: effect of the real structure and surface chemistry on the sensor properties, Russ. Chem. Bull. 57 (2008) 1106–1125.
[189] J.H. Lee, Gas sensors using hierarchical and hollow oxide nanostructures: overview, Sens. Actuators B 140 (2009) 319–336.
[190] J.W. Fergus, Perovskite oxides for semiconductor-based gas sensors, Sens. Actuators B 123 (2007) 1169–1179.
[191] J.G. Lu, P.C. Chang, Z.Y. Fan, Quasi-one-dimensional metal oxide materials-synthesis, properties and applications, Mater. Sci. Eng. R 52 (2006) 49–91.
[192] J.W. Orton, M.J. Powell, The Hall effect in polycrystalline and powdered semiconductors, Rep. Prog. Phys. 43 (1980) 1263–1307.
[193] A. Rothschild, Y. Komem, On the relationship between the grain size and gas-sensitivity of chemo-resistive metal-oxide gas sensors with nanosized grains, J. Electroceram. 13 (2004) 697–701.
[194] A. Rothschild, Y. Komem, The effect of grain size on the sensitivity of nanocrystalline metal-oxide gas sensors, J. Appl. Phys. 95 (2004) 6374–6380.
[195] E. Comini, C. Baratto, G. Faglia, M. Ferroni, A. Vomiero, G. Sberveglieri, Quasi-one dimensional metal oxide semiconductors: preparation, characterization and application as chemical sensors, Prog. Mater. Sci. 54 (2009) 1–67.

[196] G. Korotcenkov, Gas response control through structural and chemical modification of metal oxide films: state of the art and approaches, Sens. Actuators B 107 (2005) 209–232.
[197] N. Yamazoe, K. Shimanoe, New perspectives of gas sensor technology, Sens. Actuators B 138 (2009) 100–107.
[198] M. Tiemann, Porous metal oxides as gas sensors, Chem. Eur. J. 13 (2007) 8376–8388.
[199] G. Eranna, B.C. Joshi, D.P. Runthala, R.P. Gupta, Oxide materials for development of integrated gas sensors—a comprehensive review, Crit. Rev. Solid State Mater. Sci. 29 (2004) 111–188.
[200] E. Kanazawa, G. Sakai, K. Shimanoe, Y. Kanmura, Y. Teraoka, N. Miura, N. Yamazoe, Metal oxide semiconductor N_2O sensor for medical use, Sens. Actuators B 77 (2001) 72–77.
[201] C. Wang, L. Yin, L. Zhang, D. Xiang, R. Gao, Metal oxide gas sensors: sensitivity and influencing factors, Sensors 10 (2010) 2088–2106.
[202] E. Comini, G. Faglia, G. Sberveglieri, Electrical-based gas sensing, in: E. Comini, G. Faglia, G. Sberveglieri (Eds.), Solid State Gas Sensing, Springer Science + Business Media, LLC, New York, 2009.
[203] Q. Wan, Q.H. Li, Y.J. Chen, T.H. Wang, X.L. He, J.P. Li, C.L. Lin, Fabrication and ethanol sensing characteristics of ZnO NW gas sensors, Appl. Phys. Lett. 84 (18) (2004) 3654–3656.
[204] K. Arshak, I. Gaidan, Development of a novel gas sensor based on oxide thick films, Mater. Sci. Eng. B 118 (2005) 44–49.
[205] N. Wang, Y. Cai, R.Q. Zhang, Growth of nanowires, Mater. Sci. Eng. R. Rep. 60 (1–6) (2008) 1–51.
[206] S. Choopun, N. Hongsith, E. Wongrat, Metal-oxide nanowires for gas sensors, in: X. Peng (Ed.), Nanowires – Recent Advances, Intech, USA, 2012.
[207] M. Krasovska, V. Gerbreders, V. Paskevics, A. Ogurcovs, I. Mihailova, Obtaining a well-aligned ZnO nanotube array using the hydrothermal growth method, Latv. J. Phys. Tech. Sci. 52 (5) (2015) 28–40.
[208] N. Yamazoe, New approaches for improving semiconductor gas sensors, Sens. Actuators B 5 (1991) 7–19.
[209] N. Yamazoe, Toward innovations of gas sensor technology, Sens. Actuators B 108 (2005) 2–14.
[210] Y. Shimizu, M. Egashira, Basic aspects and challenges of semiconductor gas sensors, MRS Bull. 24 (1999) 18–24.
[211] A.C. Bose, P. Thangadurai, S. Ramasamy, Grain size dependent electrical studies on nanocrystalline SnO_2, Mater. Chem. Phys. 95 (2006) 72–78.
[212] E.B. Lavik, I. Kosacki, H.L. Tuller, Y.M. Chiang, J.Y. Ying, Non stoichiometry and electrical conductivity of nanocrystalline CeO_2, J. Electroceram. 1 (1997) 7–14.
[213] M.J. Baraton, L. Merbari, Influence of the particle size on the surface reactivity and gas sensing properties of SnO_2 nanopowders, Mater. Trans. 42 (2001) 1616–1622.
[214] G.J. Li, W. Wlodarski, K. Galatsis, S.H. Moslih, J. Cole, S. Russo, N. Rockelmann, Gas sensing properties of p-type semiconducting Cr-doped TiO_2 thin films, Sens. Actuators B 83 (2002) 100–163.
[215] N. Yamazoe, N. Miura (Eds.), Some basic aspects of semiconductor gas sensors, in: Chemical Sensor Technology, vol. 4, Kodansha, Tokyo, Japan, 1992.
[216] R. Schlogl, S.B. Abd Hamid, Nanocatalysis: mature science revisited or something really new? Angew. Chem. Int. Ed. 44 (2005) 3256–3260.
[217] M. Graf, B. Diego, S. Taschini, C. Hagleitner, A. Hierlemann, H. Baltes, Metal oxide-based monolithic complementary metal oxide semiconductor gas sensor microsystem, Anal. Chem. 6 (2004) 4437–4445.

[218] W. Yin, L. Pan, T. Yang, Y. Liang, Recent advances in interface engineering for planar heterojunction perovskite solar cells, Molecules 21 (2016) 837–855.
[219] F. Anderson de Sousa, Application of Transition-Metal-Oxide-Based Nanostructured Thin Films on Third Generation Solar Cells (Thesis), Centro de Tecnologia – Universidade Federal do Ceará, Brasil, 2015.
[220] K.T. Lee, J.Y. Lee, S. Seo, L. Guo, Colored ultrathin hybrid photovoltaics with high quantum efficiency, Light Sci. Appl. 3 (2014) e215.
[221] C.D. Bailie, M.G. Christoforo, J.P. Mailoa, A.R. Bowring, E.L. Unger, W. H. Nguyen, J. Burschka, N. Pellet, J.Z. Lee, M. Gratzel, R. Noufi, T. Buonassisi, A. Salleo, M.D. McGehee, Semi-transparent perovskite solar cells for tandems with silicon and CIGS, Energy Environ. Sci. 8 (2015) 956–963.
[222] K.T. Lee, J.Y. Lee, S. Seo, L.J. Guo, Microcavity-integrated colored semitransparent hybrid photovoltaics with improved efficiency and color purity, IEEE J. Photovoltaics 5 (2015) 1654–1658.
[223] D. Bryant, P. Greenwood, J. Troughton, M. Wijdekop, M. Carnie, M. Davies, K. Wojciechowski, H.J. Snaith, T. Watson, D. Worsley, A transparent conductive adhesive laminate electrode for high-efficiency organic-inorganic lead halide perovskite solar cells, Adv. Mater. 26 (2014) 7499–7504.
[224] Y.H. Chen, C.W. Chen, Z.Y. Huang, W.C. Lin, L.Y. Lin, F. Lin, K.T. Wong, H.W. Lin, Microcavity-embedded, colour-tuneable, transparent organic solar cells, Adv. Mater. 26 (2014) 1129–1134.
[225] G.E. Eperon, D. Bryant, J. Troughton, S.D. Stranks, M.B. Johnston, T. Watson, D.A. Worsley, H.J. Snaith, Efficient, semitransparent neutral-colored solar cells based on microstructured formamidinium lead trihalide perovskite, J. Phys. Chem. Lett. 6 (2015) 129–138.
[226] M. Fukuda, K.T. Lee, J.Y. Lee, L.J. Guo, Optical simulation of periodic surface texturing on ultrathin amorphous silicon solar cells, IEEE J. Photovoltaics 4 (2014) 1337–1342.
[227] G.E. Eperon, V.M. Burlakov, A. Goriely, H.J. Snaith, Neutral color semitransparent microstructured perovskite solar cells, ACS Nano 8 (2014) 591–598.
[228] F. Guo, H. Azimi, Y. Hou, T. Przybilla, M. Hu, C. Bronnbauer, S. Langner, E. Spiecker, K. Forberich, C.J. Brabec, High-performance semitransparent perovskite solar cells with solution-processed silver nanowires as top electrodes, Nanoscale 7 (2015) 1642–1649.
[229] K.T. Lee, M. Fukuda, S. Joglekar, L.J. Guo, Colored, see-through perovskite solar cells employing an optical cavity, J. Mater. Chem. C 3 (2015) 5377–5382.
[230] Z. Li, S.A. Kulkarni, P.P. Boix, E. Shi, A. Cao, K. Fu, S.K. Batabyal, J. Zhang, Q. Xiong, L.H. Wong, N. Mathews, S.G. Mhaisalkar, Laminated carbon nanotube networks for metal electrode-free efficient perovskite solar cells, ACS Nano 8 (2014) 6797–6804.
[231] C. Roldan-Carmona, O. Malinkiewicz, R. Betancur, G. Longo, C. Momblona, F. Jaramillo, L. Camacho, H.J. Bolink, High efficiency single-junction semitransparent perovskite solar cells, Energy Environ. Sci. 7 (2014) 2968–2973.
[232] E. Della Gaspera, Y. Peng, Q. Hou, L. Spiccia, U. Bach, J.J. Jasieniak, Y.B. Cheng, Ultra-thin high efficiency semitransparent perovskite solar cells, Nano Energy 13 (2015) 249–257.
[233] W. Long, C. Qin, S. Shichao, Y. Yan, J. Lin, H. Xin, Photon harvesting, coloring and polarizing in photovoltaic cell integrated color filters: efficient energy routing strategies for power-saving displays, Nanotechnology 26 (2015) 265203.
[234] W. Zhang, M. Anaya, G. Lozano, M.E. Calvo, M.B. Johnston, H. Míguez, H.J. Snaith, Highly efficient perovskite solar cells with tunable structural color, Nano Lett. 15 (2015) 1698–1702.

[235] J.H. Lu, Y.L. Yu, S.R. Chuang, C.H. Yeh, C.P. Chen, High-performance, semitransparent, easily tunable vivid colorful perovskite photovoltaics featuring Ag/ITO/Ag microcavity structures, J. Phys. Chem. C 120 (2016) 4233–4239.
[236] J.Y. Lee, K.T. Lee, S. Seo, L.J. Guo, Decorative power generating panels creating angle insensitive transmissive colors, Sci. Rep. 4 (2014) 4192.
[237] L. Wen, Q. Chen, F. Sun, S. Song, L. Jin, Y. Yu, Theoretical design of multi-colored semi-transparent organic solar cells with both efficient color filtering and light harvesting, Sci. Rep. 4 (2014) 7036.
[238] K.-T. Lee, L.J. Guo, H.J. Park, Neutral- and multi-colored semitransparent perovskite solar cells, Molecules 21 (2016) 475–496.
[239] N.K. Elumalai, C. Vijila, R. Jose, A. Uddin, S. Ramakrishna, Metal oxide semiconducting interfacial layers for photovoltaic and photocatalytic applications, Mater. Renew. Sustain. Energy 4 (2015) 11.
[240] D. Wang, R. Kou, D. Choi, Z. Yang, Z. Nie, J. Li, L.V. Saraf, D. Hu, J. Zhang, G.L. Graff, J. Liu, M.A. Pope, I.A. Aksay, Ternary self-assembly of ordered metal oxide_graphene nanocomposites for electrochemical energy storage, ACS Nano 4 (3) (2010) 1587–1595.
[241] H. Kobayashi, S. Kawamoto, S.K. Jo, H.L. Bryant, M.W. Brechbiel, R.A. Star, Macromolecular MRI contrast agents with small dendrimers, pharmacokinetic differences between sizes and cores, Bioconjug. Chem. 14 (2) (2003) 388–394.
[242] K.N. Raymond, V.C. Pierre, Next generation, high relaxivity gadolinium MRI agents, Bioconjug. Chem. 16 (1) (2005) 3–8.
[243] C. Yang, K. Chuang, GdIII chelates for MRI contrast agents from high relaxivity to smart, from blood pool to blood-brain barrier permeable, Med. Chem. Commun. 3 (2012) 552.
[244] C.Y. Cheng, K.L. Ou, W.T. Huang, J.K. Chen, J.Y. Chang, C.H. Yang, Gadolinium-based $CuInS_2ZnS$ nanoprobe for dual-modality magnetic resonance optical imaging, ACS Appl. Mater. Interfaces 5 (10) (2013) 4389–4400.
[245] E. Terreno, D.D. Castelli, A. Viale, S. Aime, Challenges for molecular magnetic resonance imaging, Chem. Rev. 110 (5) (2010) 3019–3042.
[246] K. Inouye, R. Endo, Y. Otsuka, K. Mlyashiro, K. Keneko, T. Ishikawa, Oxygenation of ferrous ions in reversed micelle and reversed microemulsion, Proc. Am. Control Conf. 88 (8) (1982) 1465–1469.
[247] S. Rao, C.R. Houska, X-ray particle-size broadening, Acta Crystallogr. A A42 (1986) 6–13.
[248] O.L. Gobbo, K. Sjaastad, M.W. Radomski, Y. Volkov, A. Prina-Mello, Magnetic nanoparticles in cancer theranostics, Theranostics 5 (11) (2015) 1249–1263.
[249] C. Ghobril, G. Lamanna, M. Kueny-Stotz, A. Garofalo, C. Billotey, D. Felder-Flesch, Dendrimers in nuclear medical imaging, New J. Chem. 36 (2) (2012) 310–323.
[250] C. Tassa, S.Y. Shaw, R. Weissleder, Dextran-coated iron oxide nanoparticles: a versatile platform for targeted molecular imaging, molecular diagnostics, and therapy, Acc. Chem. Res. 44 (10) (2011) 842–852.
[251] D. Stanicki, L. Vander Elst, R.N. Muller, S. Laurent, Synthesis and processing of magnetic nanoparticles, Curr. Opin. Chem. Eng. 6 (2015) 7–14.
[252] C. Fang, M.Q. Zhang, Multifunctional magnetic nanoparticles for medical imaging applications, J. Mater. Chem. 16 (35) (2009) 6258–6266.
[253] S. Pinho, S. Laurent, J. Rocha, A. Roch, M.-H. Delville, L. Carlos, L. Vander Elst, R. Muller, C. Geraldes, Relaxometric studies of γ-Fe_2O_3@SiO_2 core shell nanoparticles: when the coating matters, J. Phys. Chem. C 116 (3) (2012) 2285–2291.
[254] Y.W. Jun, J.H. Lee, J. Cheon, Chemical design of nanoparticle probes for high performance magnetic resonance imaging, Angew. Chem. Int. Ed. 47 (28) (2008) 5122–5135.

[255] M. Liong, J. Lu, M. Kovochich, T. Xia, S.G. Ruehm, A.E. Nel, F. Tamanoi, J.I. Zink, Multifunctional inorganic nanoparticles for imaging, targeting, and drug delivery, ACS Nano 2 (2008) 889–896.
[256] S.C. Genet, Y. Fujii, J. Maeda, M. Kaneko, M.D. Genet, K. Miyagawa, T.A. Kato, Hyperthermia inhibits homologous recombination repair and sensitizes cells to ionizing radiation in a time- and temperature-dependent manner, J. Cell. Physiol. 228 (7) (2013) 1473–1481.
[257] S. Laurent, S. Dutz, U.O. Haefeli, M. Mahmoudi, Magnetic fluid hyperthermia: focus on superparamagnetic iron oxide nanoparticles, Adv. Colloid Interface Sci. 166 (1–2) (2011) 8–23.
[258] C.L. Dennis, A.J. Jackson, J.A. Borchers, P.J. Hoopes, R. Strawbridge, A.R. Foreman, J.V. Lierop, C. Grüttner, R. Ivkov, Nearly complete regression of tumors via collective behavior of magnetic nanoparticles in hyperthermia, Nanotechnology 20 (39) (2009) 395103.
[259] K. Turcheniuk, A.V. Tarasevych, V.P. Kukhar, R. Boukherroub, S. Szunerits, Recent advances in surface chemistry strategies for the fabrication of functional iron oxide based magnetic nanoparticles, Nanoscale 5 (22) (2013) 10729–10752.
[260] A. Singh, S.K. Sahoo, Magnetic nanoparticles: a novel platform for cancer theranostics, Drug Discov. Today 19 (4) (2014) 474–481.
[261] K. Hola, Z. Markova, G. Zoppellaro, J. Tucek, R. Zboril, Tailored functionalization of iron oxide nanoparticles for MRI, drug delivery, magnetic separation and immobilization of biosubstances, Biotechnol. Adv. 33 (6) (2015) 1162–1176.
[262] D.L. Huber, Synthesis, properties, and applications of iron nanoparticles, Small 1 (2005) 482–501.
[263] A.-H. Lu, E.L. Salabas, F. Schueth, Magnetic nanoparticles: synthesis, protection, functionalization, and applicatio, Angew. Chem. Int. Ed. 46 (2007) 1222–1244.
[264] R. Hao, R. Xing, Z. Xu, Y. Hou, S. Gao, S. Sun, Synthesis, functionalization, and biomedical applications of multifunctional magnetic nanoparticles, Adv. Mater. 22 (2010) 2729–2742.
[265] J. Gao, H. Gu, B. Xu, Multifunctional magnetic nanoparticles: design, synthesis, and biomedical applications, Acc. Chem. Res. 42 (2009) 1097–1107.
[266] P. Tartaj, M.P. Morales, T. Gonzalez-Carreño, S. Veintemillas- Verdaguer, C. J. Serna, The iron oxides strike back: from biomedical applications to energy storage devices and photoelectrochemical water splitting, Adv. Mater. 23 (2011) 5243–5249.
[267] A.K. Gupta, M. Gupta, Synthesis and surface engineering of iron oxide nanoparticles for biomedical applications, Biomaterials 26 (18) (2005) 3995–4021.
[268] C. Corot, P. Robert, J.M. Idee, M. Port, Recent advances in iron oxide nanocrystal technology for medical imaging, Adv. Drug Deliv. Rev. 58 (14) (2006) 1471–1504.
[269] Y.E.L. Koo, G.R. Reddy, M. Bhojani, R. Schneider, M.A. Philbert, A. Rehentulla, B.D. Ross, R. Kopelman, Brain cancer diagnosis and therapy with nanoplatforms, Adv. Drug Deliv. Rev. 58 (14) (2006) 1556–1577.
[270] V. Pourcelle, S. Laurent, A. Welle, N. Vriamont, D. Stanicki, L. Vander Elst, R. Muller, J. Marchand-Brynaert, Functionalization of the PEG corona of nanoparticles by clip photochemistry in water: application to the grafting of RGD ligands on PEGylated USPIO imaging agent, Bioconjug. Chem. 26 (5) (2015) 822–829.
[271] D. Stanicki, S. Boutry, S. Laurent, L. Wacheul, E. Nicolas, D. Crombez, L. Vander Elst, D.L.J. Lafontaine, R.N. Muller, Carboxy-silane coated iron oxide nanoparticles: a convenient platform for cellular and small animal imaging, J. Mater. Chem. B 2 (4) (2014) 387–397.
[272] M. Abdolahi, D. Shahbazi-Gahrouei, S. Laurent, C. Sermeus, F. Firozian, B.J. Allen, S. Boutry, R.N. Muller, Synthesis and in vitro evaluation of MR molecular imaging

probes using J591 mAb-conjugated SPIONs for specific detection of prostate cancer, Contrast Med. Mol. Imaging. 8 (2) (2013) 175–184.
[273] J.C. Leach, A. Wang, K. Ye, S. Jin, A RNA-DNA hybrid aptamer for nanoparticle-based prostate tumor targeted drug delivery, Int. J. Mol. Sci. 17 (3) (2016) 380.
[274] C. Burtea, S. Laurent, S. Delcambre, C. Sermeus, D. Flamez, M.-C. Beckers, L. Vander Elst, D.L. Eizirik, R.N. Muller, Peptide targeting of (FXYD2)γa as a highly specific biomarker of pancreatic beta cells, Contrast Media Mol. Imaging 10 (5) (2015) 398–412.
[275] S. Laurent, D. Stanicki, S. Boutry, J.C. Roy, L. Vander Elst, R.N. Muller, Development of a new molecular probe for the detection of inflammatory process, J. Mol. Biol. Mol. Imaging 2 (1) (2015) 4 (id1013).
[276] H.-M. Yang, C. Woo Park, M.-A. Woo, M. Il Kim, Y. Min Jo, H. Gyu Park, J.-D. Kim, HER2/neu antibody conjugated poly(amino acid)-coated iron oxide nanoparticles for breast cancer MR imaging, Biomacromolecules 11 (2010) 2866–2872.
[277] A. Sirelkhatim, S. Mahmud, A. Seeni, N.H.M. Kaus, L.C. Ann, S.K.M. Bakhori, H. Hasan, D. Mohamad, Review on zinc oxide nanoparticles: antibacterial activity and toxicity mechanism, Nano Micro Lett. 7 (3) (2015) 219–242.
[278] S. Stankic, S. Suman, F. Haque, J. Vidic, Pure and multi metal oxide nanoparticles: synthesis, antibacterial and cytotoxic properties, J. Nanobiotechnol. 14 (1) (2016) 73–93.
[279] T. Gordon, B. Perlstein, O. Houbara, I. Felner, E. Banin, S. Margel, Synthesis and characterization of zinc/iron oxide composite nanoparticles and their antibacterial properties, Colloids Surf. A 374 (2011) 1–8.
[280] J. Vidic, S. Stankic, F. Haque, D. Ciric, R. Le Goffic, A. Vidy, J. Jupille, B. Delmas, Selective antibacterial effects of mixed ZnMgO nanoparticles, J. Nanopart. Res. 15 (2013) 1595–1605.
[281] W. He, H.K. Kim, W.G. Wamer, D. Melka, J.H. Callahan, J.J. Yin, Photogenerated charge carriers and reactive oxygen species in ZnO/Au hybrid nanostructures with enhanced photocatalytic and antibacterial activity, J. Am. Chem. Soc. 136 (2014) 750–757.
[282] K. Zawadzka, A. Kisielewska, I. Piwoński, K. Kądzioła, A. Felczak, S. Różalska, N. Wronska, K. Lisowska, Mechanisms of antibacterial activity and stability of silver nanoparticles grown on magnetron sputtered TiO_2 coatings, Bull. Mater. Sci. 39 (2016) 57–68.
[283] R. Xiong, C. Lu, Y. Wang, Z. Zhou, X. Zhang, Nanofibrillated cellulose as the support and reductant for the facile synthesis of Fe_3O_4/Ag nanocomposites with catalytic and antibacterial activity, J. Mater. Chem. A 1 (2013) 14910–14918.
[284] B.L. Guo, P. Han, L.C. Guo, Y.Q. Cao, A.D. Li, J.Z. Kong, H.F. Zhai, D. Wu, The antibacterial activity of Ta-doped ZnO nanoparticles, Nanoscale Res. Lett. 10 (2015) 1047–1057.
[285] M. Horie, K. Fujita, H. Kato, S. Endoh, K. Nishio, L.K. Komaba, A. Nakamura, A. Miyauchi, S. Kinugasa, Y. Hagihara, E. Niki, Y. Yoshida, H. Iwahashi, Association of the physical and chemical properties and the cytotoxicity of metal oxide nanoparticles: metal ion release, adsorption ability and specific surface area, Metallomics 4 (2012) 350–360.
[286] A. Ivask, T. Titma, M. Visnapuu, H. Vija, A. Kakinen, M. Sihtmae, S. Pokhrel, L. Madler, M. Heinlaan, V. Kisand, R. Shimmo, A. Kahru, Toxicity of 11 metal oxide nanoparticles to three mammalian cell types in vitro, Curr. Top. Med. Chem. 15 (2015) 1914–1929.
[287] Y. Li, W. Zhang, J. Niu, Y. Chen, Mechanism of photogenerated reactive oxygen species and correlation with the antibacterial properties of engineered metal-oxide nanoparticles, ACS Nano 6 (6) (2012) 5164–5173.

[288] J. Chevalier, L. Gremillard, Ceramics for medical applications: a picture for the next 20 years, J. Eur. Ceram. Soc. 29 (2008) 1245–1255.
[289] G. Jayaswal, S. Dange, A. Khalikar, Bioceramic in dental implants: a review, J. Indian Postho. Soc. 10 (2010) 8–12.
[290] N. Patel, G. Piyush, A review on biomaterials: scope, applications and human anatomy significance, Int. J. Emerg. Technol. Adv. Eng. 2 (2012) 2250–2459.
[291] C. Piconi, G. Maccauro, Zirconia as a ceramic biomaterial, Biomaterials 20 (1) (1999) 1–25.

FURTHER READING

[1] A.H. Latham, M.E. Williams, Controlling transport and chemical functionality of magnetic nanoparticles, Acc. Chem. Res. 41 (3) (2008) 411–420.
[2] F.M. Kievit, M. Zhang, Surface engineering of iron oxide nanoparticles for targeted cancer therapy, Acc. Chem. Res. 44 (10) (2011) 853–862.
[3] N. Wang, H.J. Wang, S. Chen, Y. Ma, Z. Zhang, Study on the anticorrosion, biocompatibility, and osteoinductivity of tantalum decorated with tantalum oxide nanotube array films, ACS Appl. Mater. Interfaces 4 (2012) 4516–4523.